Journal of the Brazilian Computer Society, 2026, 32:1, doi: 10.5753/jbcs.2026.7304

Path-Relinking Heuristics for the Offshore Wind Farm Cable Routing Problem

Murilo O. Machado [**Federal University of Mato Grosso do Sul** | ***murilo.machado@ufms.br***]
Islame F. C. Fernandes [**Federal University of Bahia** | ***islame.felipe@ufba.br***]
Silvia M. D. M. Maia [**Federal University of Rio Grande do Norte** | ***silvia@dimap.ufrn.br***]

Institute of Computing, Federal University of Bahia, Av. Milton Santos, s/n - Campus de Ondina, 40.170-110, Salvador, BA, Brazil

Received: 23 December 2025 • **Accepted:** 06 July 2026 • **Published:** 19 August 2026

Abstract An important task in offshore wind farm design is connecting previously installed turbines to a substation in a way that minimizes the total cost of submarine cables. The Offshore Wind Farm Cable Routing Problem (*WFCRP*), an NP-hard graph-based optimization problem, has modeled this task. Despite recent advances, existing approaches primarily rely on localized search strategies and do not fully exploit the structural information in high-quality solutions. This paper introduces six hybrid path-relinking heuristics for the *WFCRP*, representing the first systematic application of path-relinking strategies to this problem. The proposed algorithms combine a constructive sweep heuristic, elite-solution path-relinking trajectories, and stochastic local search. An extensive experimental evaluation on 200 real-world instances with up to 120 turbines shows that the proposed methods significantly improve solution quality for small and medium-sized instances, outperforming state-of-the-art methods such as Variable Neighborhood Search and a Multi-agent Hybrid Metaheuristic.

Keywords: Offshore Wind Farm Cable Routing, Metaheuristics, Path-Relinking, Graph-Based Optimization

1 Introduction

The global transition toward low-carbon energy systems has significantly accelerated the deployment of *wind farms* as a means of sustainable electricity generation [Song *et al.*, 2024]. According to the Global Wind Energy Council (GWEC) [2025], wind power reached a cumulative installed capacity of 1136 GW worldwide by 2025, following a record year with 117 GW of new installations in 2024. Wind energy accounted for approximately 20% of all global power-sector capacity in 2024, within a context where renewables represented nearly 90% of total new generation capacity.

Offshore wind energy has emerged as an important segment due to stronger and more stable wind resources, reduced land-use conflicts, and suitability for large-scale power generation far from densely populated areas [Yang *et al.*, 2022]. Global offshore wind installations are projected to increase from 8 GW in 2024 to approximately 34 GW by 2030, raising offshore wind's share of annual global wind additions from about 7% to nearly 18% by the end of the decade [Global Wind Energy Council (GWEC), 2025].

Despite its strategic importance, offshore wind farm development poses significant engineering challenges [Hou *et al.*, 2019; Pérez-Rúa and Cutululis, 2019]. Severe marine environments, complex seabed conditions, and high installation and maintenance costs demand robust and cost-efficient engineering solutions [Machado *et al.*, 2024; El Jaadi *et al.*, 2024; Amorosi *et al.*, 2024]. Among these challenges, the design of the electrical collection system, responsible for transporting the energy generated by turbines to offshore or onshore substations, stands out as a critical component affecting both the economic viability and operational reliability of offshore wind farms. Submarine cabling accounts for up to 30% of the total investment cost, making its optimization a significant concern in wind farm design [Wędzik *et al.*, 2016].

The *Offshore Wind Farm Cable Routing Problem* (*WFCRP*) models the interconnection of wind turbines through submarine cables with different capacities and costs, while satisfying electrical, topological, and spatial constraints. As an *NP-hard* graph-based optimization problem [Fischetti and Pisinger, 2018b], the *WFCRP* requires efficient algorithmic strategies capable of exploiting the structural properties of high-quality solutions. In this context, metaheuristic frameworks that systematically combine elite solutions represent a promising direction, particularly for large-scale and highly constrained instances. To address the *WFCRP*, several solution approaches have been proposed, including Mixed-Integer Linear Programming (MILP) formulations [Fischetti and Pisinger, 2018a, 2019], *sweep* heuristics [Cazzaro *et al.*, 2020], metaheuristic methods [Cazzaro *et al.*, 2020; Rizk-Allah *et al.*, 2024; Zhang *et al.*, 2024], and multi-agent algorithms [Machado *et al.*, 2024].

While existing algorithms have demonstrated promising results, they often rely on localized search mechanisms. They may struggle to effectively exploit the structure of high-quality solutions already identified during the optimization process. In this context, path-relinking metaheuristics [Glover, 1997] offer a powerful yet underexplored alternative. Path-relinking explores trajectories between elite solutions, systematically combining their attributes to obtain new high-quality configurations, and has proven effective in a variety of complex optimization problems [Fernandes *et al.*, 2021]. However, to the best of our knowledge, no prior study has investigated path-relinking strategies for the *WFCRP*, particularly within an offshore context.

This paper bridges this gap by proposing and evaluating six hybrid path-relinking heuristics for the Offshore *WFCRP*. The proposed approach integrates the sweep heuristic [Cazzaro *et al.*, 2020], path-relinking trajectories, and local search mechanisms to efficiently explore the solution space while preserving feasibility under offshore-specific constraints. The objective is to minimize submarine cable connection costs while ensuring reliable energy flow from turbines to the substation.

Computational experiments were conducted on a benchmark set of 200 real-world offshore wind farm instances comprising up to 120 turbines, proposed by Cazzaro *et al.* [2020]. The instances are organized into small, medium, and large categories, reflecting different wind farm scales and engineering complexities. The experimental assessment focuses on solution quality and computational efficiency, including execution time and convergence behavior. The proposed hybrid path-relinking algorithms are compared among themselves and against state-of-the-art approaches for the *WFCRP*, namely Variable Neighborhood Search (VNS) [Cazzaro *et al.*, 2020] and the Multi-Agent Hybrid Metaheuristic (MAHM) [Machado *et al.*, 2024]. All comparative analyses are supported by nonparametric statistical tests to ensure the significance of observed differences. Source codes are available at `https://github.com/metaheuristicspathrelinking-art/WFCRP.git`.

The main contributions of this work are threefold. First, it introduces the first comprehensive application of path-relinking metaheuristics to the WFCRP in an offshore engineering context. Second, it proposes and systematically evaluates multiple hybrid variants tailored to the constraints of submarine cable routing. Third, it provides an extensive experimental assessment based on real-world offshore wind farm data, offering practical insights for both researchers and offshore engineers.

The remainder of this paper is organized as follows. Section 2 reviews related work on offshore wind farm cable routing and optimization. Section 3 formally defines the *WFCRP*. Section 4 presents the proposed path-relinking methodologies and their variants. Section 5 reports the computational experiments and statistical analyses. Section 6 concludes the paper and outlines directions for future research.

2 Related work

This section reviews recent state-of-the-art studies on the *WFCRP*. Section 2.1 reviews formulations and exact algorithms, and section 2.2 details heuristic algorithms.

2.1 Formulations and exact algorithms for offshore cable connection

The literature includes various formulations for cable connections in offshore wind farms, most of which are based on MILP models. Existing exact algorithms are inherently dependent on the adopted formulation. Pérez-Rúa and Cutululis [2019] reviewed these formulations and proposed a taxonomy distinguishing between cable sizing and network routing models. For cable sizing, the authors compared static, dynamic load cycle, and full time-series approaches. Regarding network models, they classified and evaluated optimization algorithms (including heuristics, metaheuristics, and exact approaches) for designing collection systems, determining offshore substation locations, connecting turbines, and linking offshore substations to onshore points.

Existing formulations and exact algorithms have considered costs, power losses, capacity constraints, reliability, and obstacles in the area, among other aspects of wind farms. Bauer and Lysgaard [2015] formulated the problem as a planar vehicle routing model with hop-indexed constraints, solving real-world instances with up to 51 turbines. Fischetti and Pisinger [2018b] introduced a directed tree-based MILP formulation that minimizes connection costs. Formulations have also considered cable failure risks, transformer technologies, and the joint optimization of turbine placement, cable routing, and foundation design [Fischetti and Pisinger, 2018a, 2019]. Other contributions explicitly accounted for infrastructure and power-loss costs across multiple cable types, and the benefits of jointly optimizing network topology and cable cross-sections [Cerveira *et al.*, 2016; Wędzik *et al.*, 2016]. More recently, Alencar *et al.* [2026] introduced a flexible routing framework that decouples topological and geometric constraints, reducing the number of cable-crossing constraints while preserving near-optimal feasible solutions.

Pérez-Rúa *et al.* [2019] proposed a model that simultaneously determines cable cross-sections and network connections, considering both costs and power losses in the objective function. Their formulation incorporates detailed electrical characteristics and has been validated on real-world wind farms. Klein and Haugland [2019] developed an obstacle-aware integer linear model that explicitly avoids seabed obstacles and prohibits cable crossings, and showed that incorporating geophysical constraints increases costs and ensures feasible layouts. The formulation proposed by Cazzaro and Pisinger [2022] handles obstacles and boundaries using visibility graphs, allowing a connection between two turbines if and only if they are mutually visible (i.e., no obstacle lies between them). The authors focused on balanced solutions in which the number of turbines in each root-branch differs by at most one.

The simultaneous optimization of turbine placement and cable connections has been extensively explored in the literature. The study presented by Fischetti and Fischetti [2022] combined these optimization problems in a single-objective formulation, with revenue maximization as the objective function. The authors further strengthen this formulation by introducing a class of inequalities derived from the clique structure and solved the problem via a branch-and-bound algorithm. Cazzaro *et al.* [2023] also proposed a single-objective formulation, which maximizes revenues from energy production while subtracting cabling costs. The authors demonstrated that this combined approach reduced costs by 10%. In the multi-objective context, Tao *et al.* [2020] introduced a bi-level framework, where the outer layer focuses on turbine placement to maximize profit, capacity factor, and power quality, while the inner layer determines the cable connection to minimize costs. He *et al.* [2024] presented an MILP multi-objective formulation to minimize cable costs and maximize energy production.

2.2 Heuristic algorithms for offshore cable connection

Several existing works have employed heuristics and metaheuristics to address cable connection problems in offshore wind farms. Pillai *et al*. [2015] utilized a genetic algorithm combined with a minimum spanning tree method to minimize cable length and costs. Jin *et al*. [2019] used a particle swarm optimization to deal with scenarios considering the power loss cost. Rizk-Allah *et al*. [2024] proposed an improved equilibrium optimization algorithm emphasizing topology optimization. Studies that considered the simultaneous optimization of turbine placement and cable connection have used particle swarm optimization [Hou *et al*., 2016; Zhang *et al*., 2024], gradient-free search [Pérez-Rúa and Cutululis, 2022], *VNS* [Cazzaro *et al*., 2023], hyper-heuristics [Butterwick *et al*., 2023], and multi-objective genetic algorithms [Tao *et al*., 2020; He *et al*., 2024].

Cazzaro *et al*. [2020] introduced a constructive multi-start heuristic known as *Sweep*. This heuristic generates a set of feasible solutions by partitioning the set of turbines and computing a minimum spanning tree for each partition. The authors also investigated five metaheuristics: Simulated Annealing, Tabu Search, Genetic Algorithm, Ant Colony Optimization, and *VNS*. Among these metaheuristics, *VNS* demonstrated the best overall performance on real-world instances involving up to 120 turbines.

Machado *et al*. [2024] proposed the *Multi-Agent Hybrid Metaheuristic* (*MAHM*), a hybrid algorithm that combines the MILP operator presented in Fischetti and Pisinger [2018b] model with the best-performing metaheuristics presented in Cazzaro and Pisinger [2022]. *MAHM* employs a multi-agent architecture inspired by Particle Swarm Optimization, where autonomous agents iteratively apply metaheuristic strategies (*VNS*, Simulated Annealing, Tabu Search, and Informed Search). The MILP component locally refines partial solutions, enhancing convergence toward high-quality configurations. Experiments on 200 benchmark instances demonstrated that *MAHM* significantly outperformed the *VNS*.

Despite these advances in modeling and metaheuristic applications for offshore wind farm cable connection, no existing work in the literature has explored approaches based on path-relinking metaheuristics. This work fills this gap by proposing and evaluating six novel hybrid algorithms that integrate path-relinking with established heuristics for offshore cable connection.

3 Offshore Wind Farm Cable Routing Problem

The *WFCRP* models the electrical connections between wind turbines and a collector substation utilizing submarine cables. The positions of the turbines are predetermined in the open sea, while the substation's location may be onshore or offshore. The submarine cables vary in terms of cost and transmission capacity. Capacity concerns the amount of energy a cable supports, which increases with the costs. The goal is to connect all turbines to the substation using the available cables, ensuring the energy flow from the turbines to the substation. The objective function is to minimize the total cable connection cost.

In this study, the offshore *WFCRP* uses the directed tree-based formulation proposed by Fischetti and Pisinger [2018b]. Although the problem is *NP-hard*, this formulation reflects the fundamental design choices required in offshore wind farms. Given the turbines' and substation positions, the cable connection forms a tree structure rooted at the substation. Variants involving multiple substations or geographic obstacles are not considered here, since the benchmark instances in this work follow the same assumptions as in Cazzaro *et al*. [2020].

The problem is defined on a directed graph $G(V, A)$, where V is the set of vertices and A is the set of arcs. The vertex set is defined as $V = V_T \cup \{V_0\}$, where V_T represents the set of turbines (non-root vertices) and V_0 denotes the substation (root vertex). The maximum number of incoming cables at V_0 is C. The arc set is defined as $A = \{(i, j) \in V \times V : i \in V_T,\ j \in V,\ i \neq j\}$, representing all admissible submarine connections. In this formulation, arcs are allowed between turbines and from turbines to the substation, while no arcs originate from the substation node V_0. The direction of each arc represents the energy flow.

A set of submarine cable types Γ is available, where each cable $\gamma \in \Gamma$ is characterized by a unit cost $u_\gamma \geq 0$ and a capacity $k_\gamma \geq 0$. The cost of assigning cable γ to arc (i, j) is $c_{ij}^{\gamma} = u_\gamma \cdot \text{dist}(i, j)$, with $\text{dist}(i, j)$ denoting the Euclidean distance between the endpoints. This distance-based cost reflects the installation expense of submarine cables in offshore environments, which is a substantial fraction of the total project investment. *WFCRP* constraints capture engineering requirements of offshore cable connections, such as flow conservation, cable capacity limits, and cable crossings prevention.

Figure 1 illustrates the *WFCRP* model for the offshore wind farm project RJ-04, situated approximately 41 km off the coast of the State of Rio de Janeiro, Brazil (coordinates $2°38'22''S$ and $41°28'59''W$) [Sathler *et al*., 2025]. Figure 1(a) shows the RJ-04 project, consisting of 188 turbines, each with a capacity of 15 MW, and one onshore substation. Figure 1(b) illustrates a feasible solution of the *WFCRP* that utilizes three types of cables (blue, red, and black) to support the energy generated by 5, 7, and 12 turbines, respectively.

Table 1 describes the variables and expressions (1)-(11) presents the *MILP* formulation of the offshore *WFCRP* [Machado *et al*., 2024].

Table 1. Decision variables of the WFCRP formulation.

Variable	Description
$x_{ij}^{\gamma} \in \{0, 1\}$	$x_{ij}^{\gamma} = 1$ if cable γ links turbines i and j; otherwise $x_{ij}^{\gamma} = 0$.
$f_{ij} \geq 0$	Energy flow from turbine i to j.
$y_{ij} \in \{0, 1\}$	$y_{ij} = 1$ if there is a cable between turbines i and j; otherwise $y_{ij} = 0$.

$$\min \sum_{i,j \in V} \sum_{\gamma \in \Gamma} c_{ij}^{\gamma} x_{ij}^{\gamma} \tag{1}$$

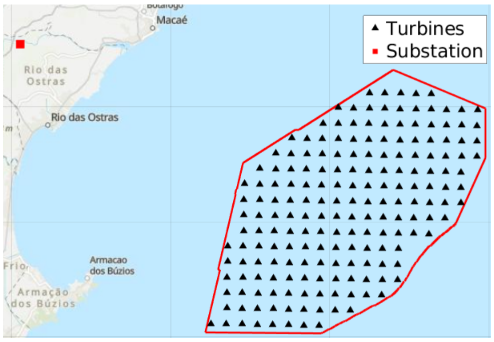

(a) RJ-04 offshore wind farm (Rio de Janeiro - Brazil) [Sathler *et al.*, 2025]

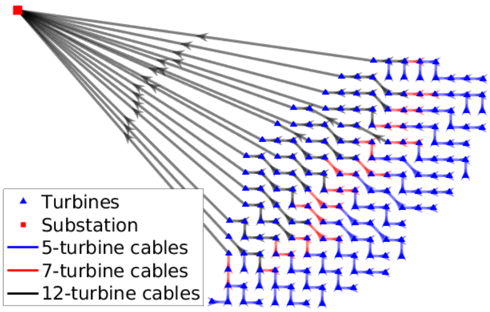

(b) A WFCRP feasible solution

Figure 1. The *WFCRP* model for a real-world offshore wind farm

$$\sum_{\gamma \in \Gamma} x_{ij}^{\gamma} = y_{ij}, \quad \forall (i,j) \in A \tag{2}$$

$$\sum_{i \in V : i \neq j} (f_{ji} - f_{ij}) = P_j, \quad \forall j \in V_T \cup \{V_0\} \tag{3}$$

$$\sum_{\gamma \in \Gamma} k_{\gamma} x_{ij}^{\gamma} \geq f_{ij}, \quad \forall (i,j) \in A \tag{4}$$

$$\sum_{j \in V : j \neq h} y_{hj} = 1, \quad \forall h \in V_T \tag{5}$$

$$\sum_{j \in V} y_{hj} = 0, \quad h = V_0 \tag{6}$$

$$\sum_{i \in V} y_{ih} \leq C, \quad h = V_0 \tag{7}$$

$$y_{ij} + y_{ji} + y_{hk} + y_{kh} \leq 1, \quad \forall ((i,j),(h,k)) \in \Theta \tag{8}$$

$$x_{ij}^{\gamma} \in 0,1, \quad (i,j) \in A,\ \gamma \in \Gamma \tag{9}$$

$$y_{ij} \in 0,1, \quad (i,j) \in A \tag{10}$$

$$f_{ij} \geq 0, \quad (i,j) \in A \tag{11}$$

Expression (1) is the objective function to minimize the total cost associated with a cable connection. Constraints (2) ensure that no more than one cable type is chosen between any two nodes. Constraints (3) enforce flow conservation, where P_j denotes the power generated by turbine $j \in V_T$. For the substation node V_0, P_{V_0} is defined as the negative value equal to the total power entering V_0, so that the flow conservation constraint is also satisfied at the root node. Constraints (4) ensure that the flow along arc (i,j) does not exceed the capacity of the cable in this arc. Additionally, constraints (5) ensure that each turbine is connected to exactly one successor, while constraints (6) prevent cables from leaving the substation. Constraints (7) limit the number of incoming cables at the substation. Constraints (8) prohibit cable crossings, where $\Theta \subset A \times A$ denotes the set of intersecting arc pairs. Constraints (9)–(11) specify the domains for the decision variables.

4 A path-relinking approach for the *WFCRP*

This section presents the proposed path-relinking algorithms for the *WFCRP*. Section 4.1 introduces the generic path-relinking procedure. Section 4.2 details the path-relinking trajectory for the *WFCRP*. Section 4.3 presents solution initialization. Section 4.4 proposes six path-relinking variants.

4.1 The generic path-relinking metaheuristic

The path-relinking metaheuristic [Glover, 1997] explores trajectories connecting high-quality solutions in the search space by progressively introducing attributes of one solution into another. Attributes are the basic elements of feasible solutions, such as the vertices or edges of a graph.

Given a *starting* solution s and a *target* solution t, the algorithm constructs a *trajectory* $s = \psi(1), \ldots, \psi(r) = t$ of solutions, where $\psi(k)$ is the k-th *intermediate solution*, $k = 1, ..., r-1$, and r is the trajectory's length. At each step, the method selects a move that introduces one or more attributes of t into the current solution $\psi(k)$. These moves reduce the distance, or *dissimilarity*, between $\psi(k)$ and t. The set $M(\psi(k), t)$ contains all feasible moves m such that applying m to $\psi(k)$, denoted $\psi(k) \oplus m$, yields a new solution $\psi(k+1)$ that is closer to t in terms of attribute similarity. As the process advances and the solutions become increasingly similar, the number of possible moves gradually decreases, i.e., $|M(\psi(k+1), t)| < |M(\psi(k), t)|$.

Algorithm 1: The generic path-relinking metaheuristic

```
Procedure PR(s, t)
    ψ* ← best of {s, t}
    k ← 1
    ψ(1) ← s
    while M(ψ(k), t) ≠ ∅ do
        choose m ∈ M(ψ(k), t)
        ψ(k+1) ← ψ(k) ⊕ m
        if ψ(k+1) is better than ψ* then
            ψ* ← ψ(k+1)
        end
        k ← k + 1
    end
    return ψ*
```

Algorithm 1, adapted from Fernandes *et al*. [2021], outlines the generic path-relinking metaheuristic employed in this study. The procedure receives s and t as input parameters. Line 2 selects the best solution between s and t according to the objective function and assigns it to ψ^*. Line 3 sets k to 1 and line 4 initializes the first solution of the path-relinking trajectory, $\psi(1) = s$. The loop between lines 5 and 12 iteratively constructs intermediate solutions until $\psi(k)$ reaches t, i.e., when $M(\psi(k), t) = \emptyset$. At each iteration, line 6 selects a move $m \in M(\psi(k), t)$. The definition of $M(\psi(k), t)$ and the selection strategy of m are problem-specific implementation issues detailed in Section 4.2. Line 7 then applies the selected move to generate the next solution, $\psi(k+1) = \psi(k) \oplus m$. Line 8 verifies whether $\psi(k+1)$ is better than the best solution found so far ψ^*, according to the objective function. In this case, line 9 sets ψ^* to $\psi(k+1)$. Finally, line 13 returns ψ^*, corresponding to the best solution identified along the path-relinking trajectory.

Numerous methodologies have been proposed for implementing path-relinking [Fernandes *et al*., 2021], demonstrating significant efficacy in solving several optimization problems [Laguna *et al*., 2025]. This metaheuristic has been successfully hybridized with various techniques, including Local Search [Ribeiro and Resende, 2012], GRASP [Resendel and Ribeiro, 2005], hyper-heuristics [Simões *et al*., 2023], and Multi-Agent Systems [Machado *et al*., 2024; Fernandes, 2022]. The hybridization of path-relinking with these approaches has significantly enhanced the quality of solutions and improved problem-solving capabilities.

4.2 Path-relinking trajectory

This study employs Algorithm 1 to generate path-relinking trajectories for the *WFCRP*. Feasible solutions are encoded as the list of arcs that define the solution. Set $M(\psi(k), t)$ is the list of arcs present in t but not in $\psi(k)$. At the beginning of the procedure, when $k = 1$ and $s = \psi(1)$, $M(\psi(1), t)$ is computed by scanning the arcs of t and inserting into $M(\psi(1), t)$ those not contained in $\psi(1)$.

At each iteration $k = 1, \ldots, r-1$, line 6 selects an arc $m \in M(\psi(k), t)$. The selection strategy prioritizes arcs $m = (i, j)$ such that i is a leaf vertex in $\psi(k)$. A leaf i is a vertex with a unique incident arc. Since $\psi(k)$ is a tree, it necessarily contains at least one leaf vertex. If there exists an arc $m = (i, j) \in M(\psi(k), t)$ such that i is a leaf in $\psi(k)$, the algorithm selects the first such arc in the list. Otherwise, it selects the first arc in $M(\psi(k), t)$. This strategy favors preserving the tree structure and helps avoid infeasible solutions. Since all non-root vertices of $\psi(k)$ have exactly one outgoing arc, let $m' = (i, h)$ be the arc outgoing from i in $\psi(k)$, where $j \neq h$. Line 7 generates $\psi(k+1)$ by inserting arc $m = (i, j)$ into $\psi(k)$ and removing arc $m' = (i, h)$, thereby maintaining the tree structure. The move set is updated as $M(\psi(k+1), t) = M(\psi(k), t) \setminus \{m\}$.

For each new solution $\psi(k+1)$, feasible cables are assigned to the arcs according to the corresponding energy flow. Cable assignment is performed by applying a shortest-path procedure from each turbine to the substation. The number of times each arc is visited determines the flow through that arc. The cheapest cable type capable of supporting that flow is selected. If no cable type supports that flow, the solution is infeasible.

The construction of the path-relinking trajectory ensures that all intermediate solutions preserve a tree structure. Besides, cable assignment ensures that the flows do not exceed the cables' capacity. It remains only to verify that there are no cable crossings and that the number of cables entering the substation does not exceed C. Verification of cable crossings considers that each arc is a line segment defined by the coordinates of incident turbines. Cable crossings are detected by solving a linear system derived from these coordinates [Jin *et al*., 2019]. Let two arcs (i_1, j_1) and (i_2, j_2), where (p_{i_1}, q_{i_1}) and (p_{j_1}, q_{j_1}) are the coordinates of turbines i_1 and j_1, respectively, and (p_{i_2}, q_{i_2}) and (p_{j_2}, q_{j_2}) are the coordinates of turbines i_2 and j_2, respectively. Two coefficients β_1 and β_2 are introduced such that expression (12) is satisfied. Expression (12) defines a linear system that can be rewritten in matrix form and solved using determinants. A crossing between arcs (i_1, j_1) and (i_2, j_2) occurs if and only if $\beta_1 \in [0, 1]$ and $\beta_2 \in [0, 1]$. In this case, the solution is infeasible and discarded during path generation.

$$\begin{cases} \beta_1 p_{i_1} + (1 - \beta_1) p_{j_1} = \beta_2 p_{i_2} + (1 - \beta_2) p_{j_2} \\ \beta_1 q_{i_1} + (1 - \beta_1) q_{j_1} = \beta_2 q_{i_2} + (1 - \beta_2) q_{j_2} \end{cases} \tag{12}$$

Figure 2 illustrates a path-relinking trajectory between $s = \psi(1)$ and t for a 5-turbine wind farm. Vertex F denotes the substation, and vertices A-E represent turbines. In this example, blue, red, and black cables support the energy produced by two, three, and four turbines, respectively. Initially, $M(\psi(1), t) = \{(A, D), (B, E), (C, F)\}$. The procedure selects arc (A, D) because vertex A is a leaf in $\psi(1)$, inserts it into $\psi(1)$, and removes arc (A, B), obtaining $\psi(2)$. As a result, the cable on (C, E) changes from red to blue, as it now supports the energy of turbines B and C, while (E, F) changes from black to red, supporting turbines B, C, and E. In the second iteration, $M(\psi(2), t) = \{(B, E), (C, F)\}$; the algorithm inserts (B, E) and removes (B, C), obtaining $\psi(3)$. Finally, (C, F) is inserted and (C, E) is removed, yielding $\psi(4) = t$.

4.3 Solution initialization

The *sweep* heuristic proposed by Cazzaro *et al*. [2020] generates the initial set of solutions used by the path-relinking. The *sweep* heuristic operates by scanning the set of turbines ordered according to their angle with the substation. The first step divides the turbines into subsets, referred to as turbine partition groups (*TPGs*), each corresponding to a subtree rooted at the substation. The scanning procedure is controlled by three parameters: a starting turbine, a scanning direction (clockwise or counterclockwise), and the size of the *TPGs*. Beginning from the selected starting turbine, the algorithm scans the remaining turbines according to the specified direction, grouping them into consecutive *TPGs*. The *TPG* size ranges from $I_1 = \lceil n/C \rceil$ to $I_2 = C_{\max}$, where n is the number of turbines, C is the maximum number of cable connections allowed at the substation, and $C_{\max}$ is the capacity of the largest available cable. If fewer turbines than the

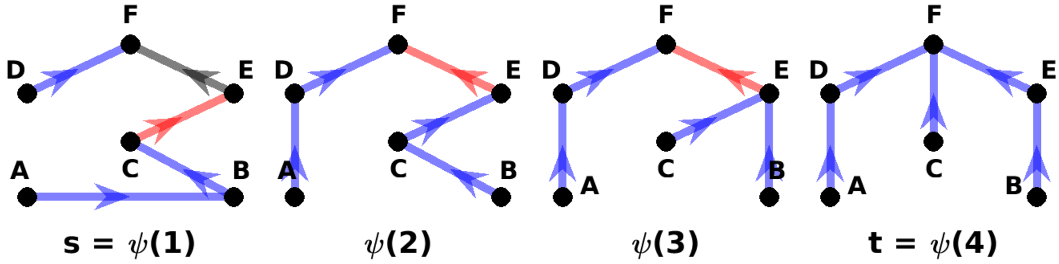

Figure 2. A path-relinking trajectory for the *WFCRP*

predefined *TPG* size remain at the end of the scan, they form the last *TPG*.

The second step computes a minimum directed spanning tree for each *TPG*. The heuristic selects the least-cost arcs to interconnect the turbines within each group and to connect them to the substation, subject to cable capacity constraints that ensure feasible energy flow.

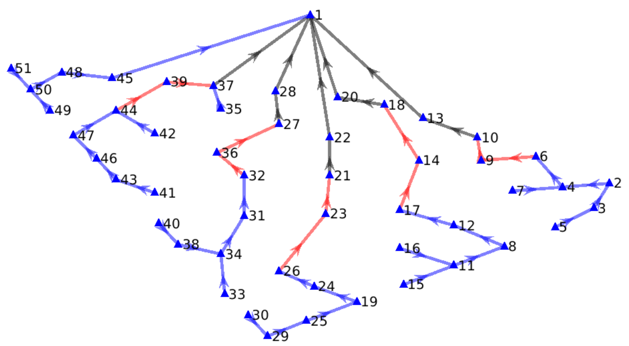

Figure 3. A solution built by the *sweep* heuristic [Machado *et al.*, 2024]

In this study, the *sweep* heuristic systematically explores all combinations of the three input parameters (starting turbine, scanning direction, and *TPG* size), producing $O(n^2)$ distinct feasible solutions. This set constitutes the initial solution pool P employed by the path-relinking algorithms described in the subsequent sections.

Figure 3 illustrates a solution generated by the *sweep* heuristic for an instance with $n = 50$ turbines, where node 1 is the substation and nodes 2 to 51 are the turbines [Machado *et al.*, 2024]. Blue, red, and black arcs indicate cables capable of supporting the energy generated by five, seven, and twelve turbines, respectively. In this example, the substation allows up to six incoming connections, and the *TPG* sizes range from $I_1 = 9$ to $I_2 = 12$. The solution was obtained by initiating the scan at turbine 2, using a clockwise direction and *TPGs* of size 9. The final *TPG* contains the remaining five turbines.

4.4 Path-relinking variants

The path-relinking variants investigated in this study consist of two phases. The first phase executes the *sweep* heuristic to generate an initial set P of feasible solutions as proposed in Cazzaro *et al.* [2020]. The second phase applies Algorithm 1 between selected pairs of solutions within P. Six algorithmic variants were implemented, differing in their strategies for selecting input solutions for the path-relinking procedure in the second phase and in the update strategy of the set P. Table 2 summarizes the path-relinking variants.

Table 2. Summary of path-relinking variants

Algorithm	Second phase
$PR1$	Path-relinking for all $s, t \in P$. Do not update P.
$PR2$	Path-relinking for all $s, t \in P$. Updates P.
$PR3$	Path-relinking between all $s \in P$ and the best solution in set P. Do not update P.
$PR4$	Path-relinking between all $s \in P$ and the best-found solution. Updates P.
$PR5$	Combines $PR2$ and a local search procedure.
$PR6$	Combines $PR4$ and a local search procedure.

Algorithm 2 outlines $PR1$. Line 1 creates the initial set P, and line 2 identifies the best solution in P, referred to as b. The loop between lines 3 and 8 executes the path-relinking algorithm for all pairs of solutions $s, t \in P$, performing the procedure in both directions: $PR(s, t)$ and $PR(t, s)$. The best solution ψ^* found along each path-relinking trajectory is determined in line 4, and line 6 updates b if a better solution is obtained.

Algorithm 2: PR1

```
1 P ← Sweep Heuristic
2 b ← the best solution in P
3 foreach s, t ∈ P do
4 |   ψ* ← PR(s, t)
5 |   if f(ψ*) < f(b) then
6 |   |   b ← ψ*
7 |   end
8 end
9 return b
```

$PR2$, $PR3$, and $PR4$ are modifications of Algorithm 2. For $PR2$, whenever a better solution ψ^* is found, line 6 inserts ψ^* into P and updates b. This ensures that subsequent iterations can use the newly inserted solution as a starting or targeting solution. Only solution pairs that have not been previously evaluated are considered, thereby avoiding redundant computations.

$PR3$ and $PR4$ differ from $PR1$ and $PR2$ in the targeting solution. The targeting solution t for $PR3$ is the best solution in the initial set P and does not change during the algorithm's execution. $PR3$ sets t to b in line 2 and then uses t to compute $PR(s, t)$ for all $s \in P$ (loop between lines 3 and 8). Unlike $PR3$, the targeting solution t for $PR4$ is the best-found solution. $PR4$ sets t to b (line 2) and updates t with ψ^* if ψ^* is better than b in line 5. Another difference between $PR3$ and $PR4$ lies in the set P. $PR3$ does not update P, while $PR4$ inserts b into P in line 6 and removes the worse solution.

Algorithm 3: Local Search

1 **Procedure** `LocalSearch(`ψ^*`)`
2   randomly select a turbine i from ψ^*
3   remove the outgoing cable of turbine i
4   generate all feasible connections of i to other turbines avoiding cycles and cable crossings
5   **foreach** *neighbor* ψ' **do**
6   assign cables along the path from i to the substation to support energy flow in ψ'
7   evaluate objective function $f(\psi')$
8   **end**
9   select neighbor ψ' with the lowest cost
10   **if** $f(\psi') < f(\psi^*)$ **then**
11         $\psi^* \leftarrow \psi'$
12   **end**
13   **return** ψ^*

$PR5$ combines $PR2$ with a stochastic single-iteration local search. Similarly, $PR6$ combines $PR4$ with the same local search mechanism. Whenever the path-relinking procedure identifies an improved solution ψ^*, it is first refined by the local search before updating b. The local search uses a 1-opt neighborhood: a turbine i is randomly selected, its outgoing cable is removed, and i is reconnected to another turbine, avoiding cable crossings and cycles. The cables along the path from i to the substation are then reassigned to accommodate the modified power flow. The best solution in the neighborhood replaces ψ^* if it improves upon it.

Algorithm 3 outlines the stochastic local search procedure applied in $PR5$ and $PR6$. Line 2 randomly selects a turbine i from the current solution ψ^*. Line 3 removes the cable exiting from turbine i. Line 4 generates all feasible reconnections of i to other turbines, avoiding cycles and cable crossings. The loop between lines 5 and 7 evaluates each neighbor by assigning cables along the path from i to the substation to support the corresponding energy flow and computing the objective function. Line 9 selects the neighbor with the lowest cost. If this neighbor improves the current solution, line 11 updates ψ^*. Finally, line 13 returns the best solution found in this local search iteration.

5 Computational experiments

All algorithms evaluated in this study were implemented in MATLAB (version 2023a) and executed sequentially in a single-threaded environment. All experiments were conducted on the same computational environment to ensure a fair comparison, using an AMD Ryzen 5-5500U processor (2.10 GHz) with 16 GB of RAM, running Ubuntu 22.04 (64-bit). The experiments aim to evaluate the effectiveness of the proposed path-relinking strategies for the *WFCRP* and compare their results with algorithms from the literature.

Section 5.1 describes the methodology (instance set, assessment protocol, and parameters tuning). Section 5.2 reports and discusses the results obtained by *PR1*, *PR2*, *PR3*, and *PR4*. Section 5.3 compares *PR5* and *PR6* with *MAHM* and *VNS*. Appendix A presents supplementary results.

5.1 Methodology

5.1.1 Instances

The tests were conducted using 200 real-world instances proposed by Cazzaro *et al*. [2020], which were organized into three categories: small, medium, and large. These instances correspond to wind farms composed of 50, 80, and 120 turbines, respectively. In total, 85 small, 75 medium, and 40 large instances were evaluated. In addition to the number of turbines, the instance generation process also considered factors such as the wind farm area, the turbine model, and the wind layout configuration. Experiments considered five real-world wind farm areas and four distinct turbine models, each with its own unique technical specifications. Each instance consisted of turbines of the same model, and the generation process included five different real-world wind farm layouts.

5.1.2 Assessment

$PR1$, $PR2$, $PR3$, and $PR4$ results concern one execution for each instance because they are non-stochastic algorithms. These algorithms are compared in terms of execution times and final solution quality. This study also reports the number of intermediate solutions better than ψ^* in line 8 of Algorithm 1. The goal is to analyze the quality of intermediate solutions found in each part of the path-relinking trajectory.

We compare results obtained by $PR5$ and $PR6$ with those by $MAHM$ [Machado *et al*., 2024] and VNS [Cazzaro *et al*., 2020] in terms of solution quality. Both algorithms were implemented by the authors. These results concern ten independent executions for each instance. As reported in Cazzaro *et al*. [2020] and Machado *et al*. [2024], both VNS and $MAHM$ exhibit most of their convergence within the first 5 minutes, with only marginal improvements thereafter. Based on this empirical evidence, we adopt a 5-minute time limit as the stopping criterion to balance computational cost and solution quality.

To ensure a fair comparison, the 5-minute runtime limit includes all algorithmic components, including the solution pool P initialization via the sweep heuristic, path-relinking trajectory generation, local search execution, and updates of the solution pool P. During execution, $PR5$ and $PR6$ iteratively evaluate pairs of solutions (s, t) selected from P, which is maintained as a list ordered according to the sweep generation. Pairs are processed deterministically following this ordering. No restart mechanism is employed, and the algorithms continuously evaluate pairs until the time limit is reached, which is the sole stopping criterion.

We analyze the distance (*GAP*) between the algorithms' results and the best-found solution. The best-found solution is the best objective function obtained using $PR5$, $PR6$, $MAHM$, and VNS for each instance. Equation (13) computes *GAP*, where VO is the quality of the solution found by the algorithm, and MV is the best-found solution for the corresponding instance. Lower *GAP* values indicate better results. The analysis also comprises the evolution of the objective function over the execution time.

$$GAP = \frac{(VO - MV) \times 100}{MV} \tag{13}$$

The Kruskal-Wallis test [Conover, 1999] verifies statistical differences among the results produced by $PR5$, $PR6$, $MAHM$, and VNS. The Kruskal-Wallis test has two phases. The first phase identifies the differences in solution quality produced by all algorithms. If the first phase identifies significant differences, the second phase performs one-tailed comparisons for each pair of algorithms. In this paper, the second phase of Kruskal-Wallis uses the Dunn post-hoc test. Due to the large number of instances, some results are presented as percentages of instances in which an algorithm was better (worse) than others. The Taillard proportion test [Taillard *et al.*, 2008] verifies whether these percentages differ significantly. The Kruskal-Wallis and Taillard tests used a significance level of 0.05.

5.1.3 Parameters tuning

The *irace* package López-Ibáñez *et al*. [2016] tuned the parameters used by *VNS* and *MAHM*. The *irace* used 20 randomly chosen instances (15 from the small group and 5 from the medium group) as the tuning set. *VNS* used 4 neighborhoods. The parameters α_1, α_2, $\#initProbAS$, and $\#initProbTgt$ for *MAHM*, detailed in Machado *et al*. [2024], were set to 0.38, 0.55, 0.25, and 0.25, respectively. The action strategies implemented within *MAHM* use the parameters defined in Cazzaro *et al*. [2020].

5.2 Comparisons between PR1, PR2, PR3, and PR4

Figure 4 shows the percentage of instances for which each algorithm produced better solutions than the others. The algorithms produced the same solution for most instances, particularly for the large group. These instances are related to a larger objective space, hindering the algorithms from escaping local optima. Figure 4(a) compares *PR1* and *PR2*. The proportion test yielded *p-values* of 0.00 for small and medium instances, indicating that *PR2* conclusively outperformed *PR1* in these instances. There was no significant difference between *PR2* and *PR1* for large instances (*p-value*$= 0.10$), and *PR1* did not surpass *PR2* in any instance. According to Figure 4(b), *PR4* conclusively outperformed *PR3* for small and medium instances (*p-values*< 0.05), and there was no significant difference for large instances (*p-values*$= 0.09$). The superior behavior of *PR2* and *PR4* comes from updating set P and using high-quality solutions as starting and targeting points.

Figure 5 shows the average number of best intermediate solutions discovered in each part of the path-relinking trajectory. The x-axis divides the trajectory into 10 equal parts, written as a percentage; that is, the first part is the first 10% of the path, the second is from 10% to 20%, and so on. The y-axis indicates the average number of times line 9 of Algorithm 1 is

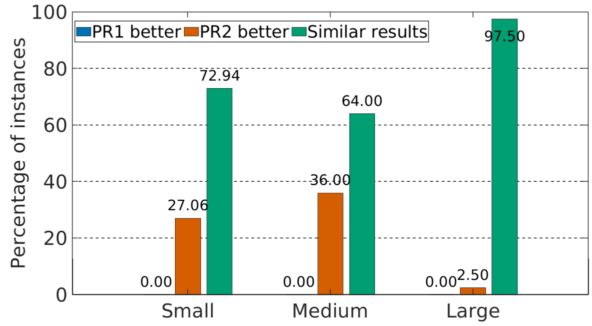

(a) *PR1 versus PR2*

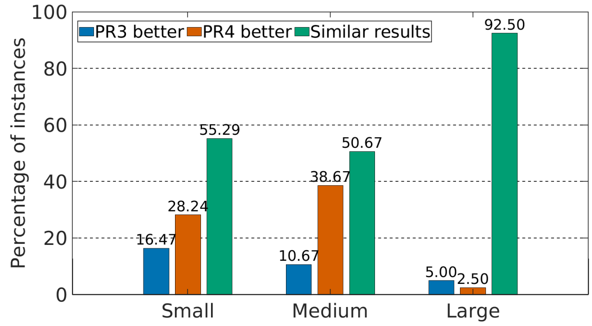

(b) *PR3 versus PR4*

Figure 4. Comparison between the solution quality produced *PR1*, *PR2*, *PR3*, and *PR4* for each group of instances

executed for each section on the x-axis. The best intermediate solutions were mainly obtained at the beginning (from 0% to 20%) and the end (from 80% to 100%) of the path-relinking trajectory. These results suggest that searching in the starting and targeting neighborhoods yields better solutions.

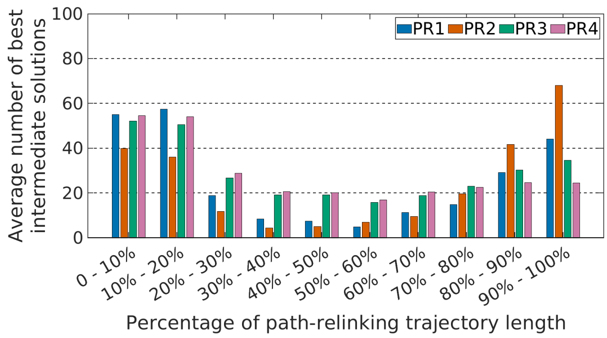

Figure 5. Distribution of best solutions within the trajectory

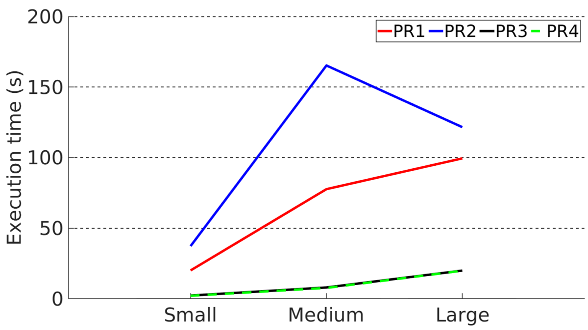

Figure 6. Execution time (in seconds)

Figure 6 shows the average execution times (in seconds) spent by the algorithms for each group of instances. As *PR1* and *PR2* build path-relinking trajectories for all pairs of solutions, they require more processing time than *PR3* and *PR4*. *PR2* requires more processing time than *PR1*, as the former computes more pairs of solutions. The execution times of *PR1*, *PR3*, and *PR4* increased with the size of the instances. *PR2* requires less processing time for large instances than for medium ones. This behavior can be explained by the nature of the solutions that *PR2* inserts into P. For large instances, *PR2* tends to generate solutions that are more similar to those already present in P, leading to reduced diversity. As a consequence, path-relinking produces shorter trajectories and fewer effective improvements in subsequent iterations, thereby reducing the overall processing time.

5.3 Comparisons between PR5, PR6, MAHM, and VNS

The first Kruskal-Wallis test indicated significant differences among the algorithms for all instances. Table 3 shows the number of instances for which the pairwise test concluded (p-*values* < 0.05) that the algorithm in the row produced a better *GAP* than the algorithm in the column. Green cells highlight comparisons where the Taillard test indicated significant differences. For most small instances, *PR5* and *PR6* performed similarly and produced a better *GAP* than *MAHM* and *VNS*. For medium instances, *PR6* was better than *PR5* and *VNS*. *MAHM* outperformed *PR5* and *PR6* for medium and large instances; *VNS* did for large instances. These results show that the solution quality produced by *PR5* and *PR6* decreases as the instance size increases. As explained earlier, the size of the objective space increases with the number of turbines, which poses difficulties to the path-relinking techniques. However, *PR5* is effective on wind farms with up to 50 turbines and *PR6* with up to 80.

Table 3. Comparison between *PR5*, *PR6*, *MAHM*, and *VNS* using Kruskal–Wallis and Taillard statistical tests.

	PR5	PR6	MAHM	VNS
Small instances				
PR5	–	6	32	58
PR6	8	–	26	61
MAHM	21	16	–	17
VNS	13	12	0	–
Medium instances				
PR5	–	3	7	21
PR6	16	–	9	31
MAHM	40	24	–	22
VNS	25	9	0	–
Large instances				
PR5	–	0	1	1
PR6	2	–	1	1
MAHM	39	35	–	2
VNS	35	21	0	–

Figure 7 presents the number of independent executions for which the algorithms produced the best-found solution (*MV*).

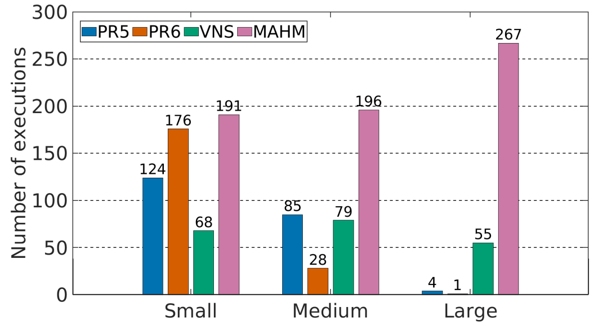

Figure 7. Number of executions for which the algorithms produced the best-found solution

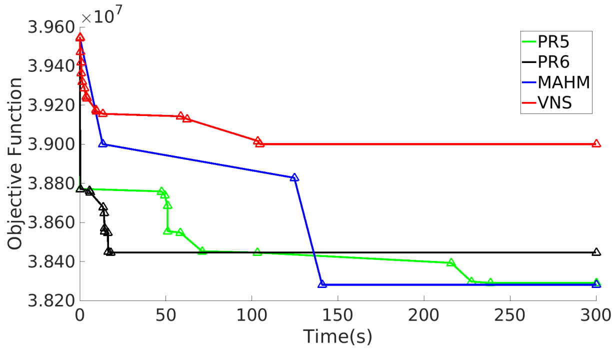

(a) Small instance (ID=33)

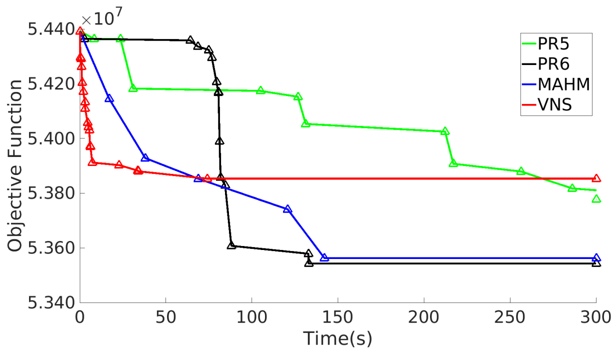

(b) Medium instance (ID=93)

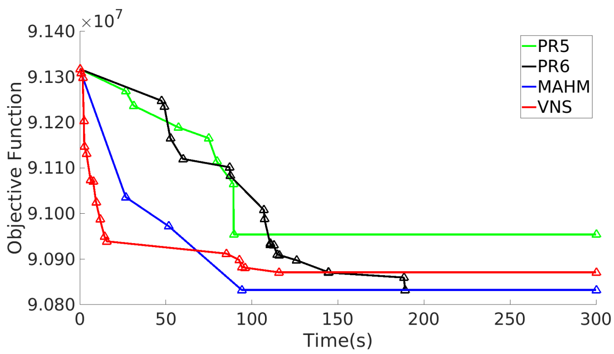

(c) Large instance (ID=172)

Figure 8. Objective function over execution time

The number of executions for which *PR5* and *PR6* produced *MV* decreases while *MAHM* increases with the instance size. *PR5* surpasses *VNS* for small and medium instances, and *PR6* does for small instances. Although *PR6* has achieved *MV* less times than *PR5* and *VNS* for medium instances, *PR6* produced the nearest solutions to *MV* on average.

Figure 8 illustrates the evolution of the objective function over execution time for representative small, medium, and large instances. In all cases, *VNS* exhibits a rapid initial improvement but stagnates early in the search, indicating a tendency to converge prematurely to local optima within the first minutes of execution. *MAHM* exhibits a more gradual convergence behavior, achieving significant improvements in the early and mid phases, but converges to a local optimum before approximately 150 seconds in all scenarios. *PR6* quickly converges for the small instance, while showing more progressive improvements for medium and large instances. *PR5* exhibits a steady improvement over time for small and medium instances, continuing to refine solutions until the final stages of execution. In contrast, for large instances, *PR5*'s improvement becomes limited after approximately 100 seconds. These results indicate that path-relinking strategies can maintain improvement over time, particularly for small and medium instances; however, their performance becomes more constrained as the problem size increases due to the expansion of the search space.

6 Conclusion and future work

This study explored the application of path-relinking heuristics to solve the *WFCRP*, with the objective function of minimizing cabling costs. Six hybrid algorithms were proposed, which combined the sweep heuristic, local search, and path-relinking techniques. Computational experiments on 200 real-world instances revealed that path-relinking strategies, particularly *PR2* and *PR4*, surpassed simpler approaches (*PR1* and *PR3*) by reusing newly computed solutions as starting and targeting points. *PR5* and *PR6* produced competitive results for small and medium-sized instances compared to state-of-the-art methods such as *MAHM* and *VNS*. However, their performance declined for larger instances due to the increased solution space. Statistical tests affirmed the effectiveness of path-relinking in enhancing solution quality, particularly during both the early and late stages of the optimization trajectory.

By advancing the state-of-the-art in *WFCRP* optimization, this study not only contributed to the academic literature but also supported the renewable energy sector in reducing infrastructure costs—a crucial step toward making wind energy more competitive and scalable.

Future work could explore several directions to enhance the proposed methods. Hybridizing path-relinking with other metaheuristics, such as genetic algorithms or simulated annealing, might further improve both exploration and exploitation capabilities for the *WFCRP*. Additionally, incorporating advanced machine learning techniques could dynamically guide the selection of starting and targeting solutions in path-relinking, enhancing efficiency for large-scale instances. These advancements would strengthen the practical relevance of path-relinking metaheuristic and contribute to developing more sustainable and cost-effective wind energy infrastructure.

Declarations

Authors' Contributions

Murilo O. Machado contributed to the conceptualization, data curation, formal analysis, investigation, methodology, software, and writing – original draft of this study. **Islame F. C. Fernandes** contributed to the conceptualization, data curation, formal analysis, funding acquisition, project administration, supervision, validation, writing – original draft, and writing – review & editing. **Silvia M. D. M. Maia** contributed to the conceptualization, formal analysis, validation, and writing – original draft. **Murilo O. Machado** is the main contributor and writer of this manuscript. All authors read and approved the final manuscript.

Competing interests

The authors declare that they have no competing interests.

Acknowledgements

This research was supported by the Brazilian Federal Agency for Support and Evaluation of Graduate Education (CAPES/Brazil); the National Council for Scientific and Technological Development (CNPq), Brazil, under grant 402842/2023-5; Federal University of Bahia; Federal University of Rio Grande do Norte; and Federal University of Mato Grosso do Sul.

Availability of data and materials

The datasets (and/or softwares) generated and/or analysed during the current study are available at `https://github.com/metaheuristicspathrelinking-art/WFCRP.git`.

References

Alencar, M. S., Göçmen, T., and Cutululis, N. A. (2026). Flexible cable routing framework for wind farm collection system optimization. *European Journal of Operational Research*, 329(3):1037–1051. DOI: 10.1016/j.ejor.2025.07.069.

Amorosi, L., Fischetti, M., Paradiso, R., and Roberti, R. (2024). Optimization models for the installation planning of offshore wind farms. *European Journal of Operational Research*, 315(3):1182–1196. DOI: 10.1016/j.ejor.2024.01.011.

Bauer, J. and Lysgaard, J. (2015). The offshore wind farm array cable layout problem: a planar open vehicle routing problem. *Journal of the Operational Research Society*, 66(3):360–368. DOI: 10.1057/jors.2013.188.

Butterwick, T., Kheiri, A., Lulli, G., Gromicho, J., and Kreeft, J. (2023). Application of selection hyper-heuristics to the simultaneous optimisation of turbines and cabling within an offshore windfarm. *Renewable Energy*, 208:1–16. DOI: 10.1016/j.renene.2023.03.075.

Cazzaro, D., Fischetti, M., and Fischetti, M. (2020). Heuristic algorithms for the wind farm cable routing problem. *Applied Energy*, 278:115617. DOI: doi.org/10.1016/j.apenergy.2020.115617.

Cazzaro, D., Koza, D. F., and Pisinger, D. (2023). Combined layout and cable optimization of offshore wind farms. *European Journal of Operational Research*, 311(1):301–315. DOI: 10.1016/j.ejor.2023.04.046.

Cazzaro, D. and Pisinger, D. (2022). Balanced cable routing for offshore wind farms with obstacles. *Networks: An International Journal*, 80(4):386–406. DOI: 10.1002/net.22100.

Cerveira, A., de Sousa, A., Pires, E. S., and Baptista, J. (2016). Optimal cable design of wind farms: The infrastructure and losses cost minimization case. *IEEE Transactions on Power Systems*, 31(6):4319–4329. DOI: 10.1109/TPWRS.2016.2521700.

Conover, W. J. (1999). *Practical nonparametric statistics*, volume 350. John Wiley & Sons. DOI: 10.2307/1402479.

El Jaadi, M., Haidi, T., and Belfqih, A. (2024). Advancements in wind farm layout optimization: a comprehensive review of artificial intelligence approaches. *TELKOMNIKA (Telecommunication Computing Electronics and Control)*, 22(3):763–772. DOI: 10.12928/telkomnika.v22i3.25609.

Fernandes, I. F., Goldbarg, E. F., Maia, S. M., and Goldbarg, M. C. (2021). Multi- and many-objective path-relinking: A taxonomy and decomposition approach. *Computers & Operations Research*, 133:105370. DOI: 10.1016/j.cor.2021.105370.

Fernandes, I. F. d. C. (2022). *Hybridizing metaheuristics for multi- and many-objective problems in a multi-agent architecture*. PhD thesis, Universidade Federal do Rio Grande do Norte. Available at:`https://repositorio.ufrn.br/bitstreams/cfd61273-14e9-49e7-848f-4bf7a37700c3/download`.

Fischetti, M. and Fischetti, M. (2022). Integrated layout and cable routing in wind farm optimal design. *Management Science*, 69(4):2147–2164. DOI: 10.1287/mnsc.2022.4470.

Fischetti, M. and Pisinger, D. (2018a). Mixed integer linear programming for new trends in wind farm cable routing. *Electronic Notes in Discrete Mathematics*, 64:115–124. DOI: 10.1016/j.endm.2018.01.013.

Fischetti, M. and Pisinger, D. (2018b). Optimizing wind farm cable routing considering power losses. *European Journal of Operational Research*, 270(3):917–930. DOI: 10.1016/j.ejor.2017.07.061.

Fischetti, M. and Pisinger, D. (2019). Mathematical optimization and algorithms for offshore wind farm design: An overview. *Business & Information Systems Engineering*, 61(4):469–485. DOI: 10.1007/s12599-018-0538-0.

Global Wind Energy Council (GWEC) (2025). Global Wind Report 2025. Available at:`https://www.gwec.net/reports/globalwindreport/2025`.

Glover, F. (1997). Tabu search and adaptive memory programming—advances, applications and challenges. *Interfaces in Computer Science and Operations Research: Advances in Metaheuristics, Optimization, and Stochastic Modeling Technologies*, pages 1–75. DOI: 10.1007/978-1-4615-4102-8_1.

He, J., Ge, M., Žarković, S. D., Li, Z., and Hilber, P. (2024). A novel integrated optimization method of micrositing and cable routing for offshore wind farms. *Energy*, 306:132443. DOI: 10.1016/j.energy.2024.132443.

Hou, P., Hu, W., and Chen, Z. (2016). Optimisation for offshore wind farm cable connection layout using adaptive particle swarm optimisation minimum spanning tree method. *IET Renewable Power Generation*, 10(5):694–702. DOI: 10.1049/iet-rpg.2015.0340.

Hou, P., Zhu, J., Ma, K., Yang, G., Hu, W., and Chen, Z. (2019). A review of offshore wind farm layout optimization and electrical system design methods. *Journal of Modern Power Systems and Clean Energy*, 7(5):975–986. DOI: 10.1007/s40565-019-0550-5.

Jin, R., Hou, P., Yang, G., Qi, Y., Chen, C., and Chen, Z. (2019). Cable routing optimization for offshore wind power plants via wind scenarios considering power loss cost model. *Applied Energy*, 254:113719. DOI: 10.1016/j.apenergy.2019.113719.

Klein, A. and Haugland, D. (2019). Obstacle-aware optimization of offshore wind farm cable layouts. *Annals of Operations Research*, 272(1):373–388. DOI: 10.1007/s10479-017-2581-5.

Laguna, M., Martí, R., Martínez-Gavara, A., Pérez-Peló, S., and Resende, M. G. (2025). Greedy randomized adaptive search procedures with path relinking. an analytical review of designs and implementations. *European Journal of Operational Research*, 327(3):717–734. DOI: 10.1016/j.ejor.2025.02.022.

López-Ibánez, M., Dubois-Lacoste, J., Cáceres, L. P., Birattari, M., and Stützle, T. (2016). The irace package: Iterated racing for automatic algorithm configuration. *Operations Research Perspectives*, 3:43–58. DOI: 10.1016/j.orp.2016.09.002.

Machado, M. O., Fernandes, I. F. C., Maia, S. M. D. M., and Goldbarg, E. F. G. (2024). A hybrid multi-agent metaheuristic for the offshore wind farm cable routing problem. *Expert Systems with Applications*, page 124668. DOI: 10.1016/j.eswa.2024.124668.

Pérez-Rúa, J.-A. and Cutululis, N. A. (2019). Electrical cable optimization in offshore wind farms—a review. *IEEE Access*, 7:85796–85811. DOI: 10.1109/ACCESS.2019.2925873.

Pérez-Rúa, J.-A. and Cutululis, N. A. (2022). A framework for simultaneous design of wind turbines and cable layout in offshore wind. *Wind Energy Science*, 7(2):925–942. DOI: 10.5194/wes-7-925-2022.

Pérez-Rúa, J.-A., Stolpe, M., and Cutululis, N. A. (2019). Integrated global optimization model for electrical cables in offshore wind farms. *IEEE Transactions on Sustainable Energy*, 11(3):1965–1974. DOI: 10.1109/TSTE.2019.2948118.

Pillai, A. C., Chick, J., Johanning, L., Khorasanchi, M., and De Laleu, V. (2015). Offshore wind farm electrical cable layout optimization. *Engineering Optimization*, 47(12):1689–1708. DOI: 10.1080/0305215X.2014.992892.

Resendel, M. G. and Ribeiro, C. C. (2005). GRASP with path-relinking: Recent advances and applications. *Metaheuristics: progress as real problem solvers*, pages 29–63. DOI: doi.org/10.1007/0-387-25383-1_2.

Ribeiro, C. C. and Resende, M. G. C. (2012). Path-relinking intensification methods for stochastic local search algorithms. *Journal of heuristics*, 18:193–214. DOI: 10.1007/s10732-011-9167-1.

Rizk-Allah, R. M., Snášel, V., Deng, X., Song, D., and Hassanien, A. E. (2024). Topological optimization of offshore wind farm cable routing system based on an improved equilibrium optimization algorithm. *Ocean Engineering*, 313:119539. DOI: 10.1016/j.oceaneng.2024.119539.

Sathler, K., Yeter, B., Gouveia, A., and Kolios, A. (2025). Effects of neighbouring offshore wind farms on techno-economic metrics: A case study of a brazilian offshore wind project. *Ocean Engineering*, 339:122189. DOI: doi.org/10.1016/j.oceaneng.2025.122189.

Simões, M., Bahiense, L., and Figueiredo, C. (2023). Hyper-heuristics with Path Relinking applied to the Generalised Time-Dependent ATSP in air travel. *Procedia Computer Science*, 223:35–42. DOI: 10.1016/j.procs.2023.08.211.

Song, D., Shen, G., Huang, C., Huang, Q., Yang, J., Dong, M., Joo, Y. H., and Duić, N. (2024). Review on the application of artificial intelligence methods in the control and design of offshore wind power systems. *Journal of marine science and engineering*, 12(3):424. DOI: 10.3390/jmse12030424.

Taillard, É. D., Waelti, P., and Zuber, J. (2008). Few statistical tests for proportions comparison. *European Journal of Operational Research*, 185(3):1336–1350. DOI: 10.1016/j.ejor.2006.03.070.

Tao, S., Xu, Q., Feijóo, A., and Zheng, G. (2020). Joint optimization of wind turbine micrositing and cabling in an offshore wind farm. *IEEE Transactions on Smart Grid*, 12(1):834–844. DOI: 10.1109/TSG.2020.3022378.

Wędzik, A., Siewierski, T., and Szypowski, M. (2016). A new method for simultaneous optimizing of wind farm's network layout and cable cross-sections by milp optimization. *Applied Energy*, 182:525–538. DOI: 10.1016/j.apenergy.2016.08.094.

Yang, B., Liu, B., Zhou, H., Wang, J., Yao, W., Wu, S., Shu, H., and Ren, Y. (2022). A critical survey of technologies of large offshore wind farm integration: Summary, advances, and perspectives. *Protection and Control of Modern Power Systems*, 7(1):17. DOI: 10.1186/s41601-022-00239-w.

Zhang, D., Liu, Z., Liang, Y., Li, C., Zhang, J., and Hu, G. (2024). Bilevel optimization of non-uniform offshore wind farm layout and cable routing for the refined LCOE using an enhanced PSO. *Ocean Engineering*, 299:117244. DOI: 10.1016/j.oceaneng.2024.117244.

A Supplementary results

See Tables 4-16.

Table 4. Average *GAP* to the best-found solution concerning small instances

ID	Best found solution	GAP to the best found solution				ID	Best-found solution	GAP to the best found solution			
		PR5	PR6	VNS	MAHM			PR5	PR6	VNS	MAHM
1	35325676.40	0.38	**0.26**	2.31	2.25	44	37216452.31	0.31	0.21	0.18	**0.00**
2	35424005.04	0.34	**0.08**	2.79	1.79	45	38181816.02	**0.03**	0.09	0.87	0.63
3	35384833.29	1.23	2.10	3.82	**0.74**	46	32978151.34	12.99	12.98	14.48	**12.68**
4	35401861.56	0.27	**0.10**	0.60	0.41	47	37622312.35	0.72	**0.20**	0.45	0.37
5	35761144.35	0.32	**0.31**	1.93	1.42	48	38369242.93	0.27	**0.19**	1.48	0.80
6	33034885.69	0.14	0.01	0.01	**0.00**	49	36571737.88	**0.59**	0.67	2.26	1.53
7	32768823.91	1.02	0.54	**0.06**	0.38	50	37466952.64	0.43	**0.25**	0.98	0.51
8	33362800.92	1.14	0.66	0.47	**0.00**	51	43336818.68	**0.24**	1.27	1.90	1.90
9	32458302.71	0.80	0.57	0.31	**0.02**	52	43752363.17	**0.26**	0.38	0.52	0.58
10	32229957.07	0.22	**0.01**	0.61	0.73	53	44544644.08	**0.00**	**0.00**	2.05	1.43
11	35706544.71	**0.04**	0.18	1.30	0.67	54	43599073.18	0.04	**0.01**	2.54	2.07
12	35486655.10	**0.00**	0.05	2.25	1.85	55	43867271.25	**0.19**	0.31	0.75	0.65
13	35892608.90	0.42	0.40	0.54	**0.38**	56	40411963.63	1.89	**0.41**	1.78	1.04
14	34933980.28	**0.37**	0.57	1.17	1.09	57	38882533.64	0.17	**0.15**	3.67	2.99
15	35938528.14	**0.28**	**0.28**	0.50	0.44	58	41137687.02	**0.69**	0.92	2.06	1.36
16	35234097.41	0.27	**0.13**	2.34	1.72	59	39424664.32	**0.07**	**0.07**	2.05	1.74
17	29466349.22	1.00	0.22	1.32	**0.00**	60	39703166.64	**0.68**	0.78	1.56	0.85
18	29035448.18	2.29	**1.60**	2.45	1.75	61	43558482.23	**0.39**	0.57	1.05	0.62
19	29692763.76	0.62	**0.52**	1.00	0.54	62	44284046.52	0.29	0.29	**0.00**	0.03
20	29694186.11	1.20	1.04	0.58	**0.57**	63	45518790.98	**0.01**	0.02	0.54	0.08
21	31284646.79	**0.00**	0.11	0.64	0.51	64	42048368.40	**0.00**	**0.00**	**0.00**	**0.00**
22	30714562.56	**0.22**	0.45	1.15	1.51	65	42461447.13	**0.00**	0.02	**0.00**	**0.00**
23	31013102.06	**0.00**	**0.00**	0.28	0.28	66	43658335.98	**0.55**	1.92	2.04	1.88
24	31730026.04	**0.00**	**0.00**	0.54	0.48	67	89582862.21	6.54	6.58	7.20	**6.12**
25	30930205.06	0.13	**0.09**	0.67	0.64	68	99728297.98	0.07	**0.06**	0.22	0.07
26	30504138.61	2.31	**2.29**	4.83	4.44	69	92574270.61	0.20	0.23	0.32	**0.12**
27	30987238.09	**0.00**	0.35	2.08	1.73	70	88092132.03	1.20	1.49	1.23	**1.05**
28	31355927.65	**0.17**	**0.17**	0.93	0.24	71	86351211.98	0.40	**0.08**	0.32	0.32
29	30651789.69	**2.45**	3.01	5.64	4.83	72	86401745.97	1.63	1.23	**0.37**	0.52
30	32306252.74	1.49	**0.35**	3.65	2.80	73	90146928.25	0.60	0.51	0.10	**0.00**
31	38343508.00	0.96	**0.76**	1.19	1.09	74	79119263.78	6.42	5.56	5.58	**5.01**
32	37675621.63	1.14	**1.09**	1.85	1.24	75	84933784.82	**0.00**	**0.00**	**0.00**	**0.00**
33	38281196.41	0.39	**0.37**	1.89	0.81	76	98212386.46	**0.33**	0.51	0.86	0.91
34	38404692.43	**0.16**	0.22	1.24	0.84	77	92553547.61	6.98	7.46	7.27	**6.54**
35	33951962.91	**10.15**	10.22	13.05	10.62	78	101247237.27	0.04	**0.00**	**0.00**	**0.00**
36	33832701.27	1.16	1.16	**0.00**	**0.00**	79	94874501.19	**0.00**	0.20	0.68	0.67
37	33588161.67	**0.17**	1.04	0.94	1.03	80	93897687.26	1.03	1.03	0.82	**0.65**
38	34176044.24	0.52	0.51	0.25	**0.21**	81	93639891.77	1.85	**0.26**	1.33	1.12
39	32971434.61	**0.00**	**0.00**	0.42	0.04	82	95110065.08	0.84	0.86	1.72	**0.49**
40	34278578.58	0.59	**0.43**	1.53	1.21	83	98709507.85	**0.23**	2.20	1.56	1.51
41	38536227.93	0.10	0.12	0.06	**0.03**	84	95237160.59	**0.06**	0.17	2.44	1.25
42	38577993.65	**0.00**	0.11	0.25	0.21	85	90001549.15	**0.01**	0.40	0.40	0.36
43	38626358.24	**0.22**	**0.22**	0.66	0.51						

Table 5. Average *GAP* to the best-found solution concerning medium instances

ID	Best found solution	GAP to the best found solution				ID	Best-found solution	GAP to the best found solution			
		PR5	PR6	VNS	MAHM			PR5	PR6	VNS	MAHM
86	47126070.53	0.95	**0.18**	0.32	0.58	124	50147277.91	1.03	0.41	0.27	**0.02**
87	46838244.88	1.06	0.31	0.10	**0.00**	125	50474779.73	0.55	0.14	0.17	**0.09**
88	46946361.16	1.40	0.57	0.84	**0.23**	126	62279321.42	0.48	**0.30**	0.54	0.31
89	46937722.82	0.44	0.23	0.49	**0.17**	127	63704199.76	0.76	0.93	0.87	**0.67**
90	46748899.27	0.72	0.49	0.08	**0.02**	128	64140568.86	0.31	**0.13**	0.56	0.46
91	52448141.89	0.90	0.77	1.26	**0.73**	129	62474291.19	0.25	**0.06**	0.39	0.37
92	52284893.48	0.91	0.88	0.88	**0.62**	130	61860090.64	0.49	0.40	0.08	**0.07**
93	53140196.30	1.56	1.59	1.36	**0.52**	131	53576087.27	6.93	6.30	6.73	**6.04**
94	51615997.61	**0.04**	0.60	1.59	0.70	132	54096678.20	6.30	6.26	6.82	**4.79**
95	52446864.73	0.35	0.35	0.96	**0.26**	133	58133478.47	0.57	0.55	0.56	**0.21**
96	50545402.33	0.49	0.52	**0.15**	0.16	134	56388331.81	0.76	0.53	0.60	**0.47**
97	50780661.17	0.81	0.58	0.30	**0.14**	135	58050849.15	0.52	**0.06**	0.73	0.50
98	51590872.45	0.75	0.70	0.44	**0.06**	136	65609071.22	**0.78**	0.88	1.19	0.89
99	50330755.65	0.20	0.03	**0.00**	0.14	137	64415702.74	**0.08**	0.38	0.88	0.63
100	50763657.82	0.92	0.76	0.83	**0.64**	138	65641437.45	1.41	1.30	1.90	**1.18**
101	44589656.71	1.00	0.75	0.90	**0.57**	139	64335748.25	**0.07**	**0.07**	1.68	0.56
102	44981809.92	0.95	0.46	0.37	**0.23**	140	65679281.92	0.78	**0.75**	1.53	0.85
103	45362909.89	0.47	0.32	0.57	**0.20**	141	62221943.56	0.49	**0.14**	0.34	0.33
104	45292781.04	0.46	0.16	0.36	**0.00**	142	62454154.92	0.54	**0.15**	0.60	0.62
105	43570407.01	1.37	0.62	**0.06**	0.24	143	63339233.11	0.63	0.53	0.64	**0.19**
106	41333742.96	**0.36**	0.37	0.53	0.49	144	60798736.65	0.08	**0.00**	0.28	0.28
107	41652888.26	0.66	**0.31**	0.91	0.34	145	63256258.29	0.70	0.83	0.84	**0.66**
108	41690019.14	0.31	**0.07**	0.52	0.35	146	135471555.81	0.52	0.48	0.14	**0.00**
109	41566335.46	1.84	1.35	0.43	**0.08**	147	134250436.85	**0.17**	0.18	0.29	0.25
110	40810118.93	1.18	0.82	0.96	**0.56**	148	137809866.02	0.11	0.05	0.32	**0.00**
111	45908273.06	0.44	**0.26**	0.76	0.53	149	132717848.85	**0.12**	0.55	0.42	0.42
112	46116256.39	0.75	**0.61**	1.14	0.85	150	115535014.81	0.80	**0.49**	1.31	1.12
113	46531795.74	**0.34**	0.55	0.99	0.69	151	140195526.43	0.84	0.84	**0.08**	0.10
114	46590121.43	0.51	0.37	0.02	**0.00**	152	142434454.82	0.17	**0.05**	0.55	0.50
115	45444337.10	0.57	**0.10**	0.43	0.41	153	146691128.58	0.60	0.52	0.09	**0.06**
116	44504878.90	0.15	**0.04**	0.25	0.20	154	137052063.14	1.05	1.04	1.10	**0.85**
117	44004002.68	0.37	0.22	0.74	**0.00**	155	136396459.85	**0.00**	**0.00**	**0.00**	**0.00**
118	45055489.99	0.44	**0.21**	0.31	0.29	156	132399493.31	0.25	0.25	**0.00**	**0.00**
119	44208234.54	0.14	0.00	0.00	**0.00**	157	132524394.56	0.22	0.22	**0.00**	0.03
120	43132993.20	1.28	0.88	0.70	**0.37**	158	139763146.62	0.51	0.19	0.07	**0.02**
121	50513464.19	0.94	0.64	0.31	**0.17**	159	131880338.53	**0.01**	**0.01**	**0.01**	**0.01**
122	49875973.82	0.82	0.77	0.74	**0.47**	160	131748714.52	**0.15**	1.16	1.33	1.15
123	50387724.97	0.52	0.13	0.08	**0.01**						

Table 6. Average *GAP* to the best-found solution concerning large instances

ID	Best found solution	GAP to the best found solution				ID	Best-found solution	GAP to the best found solution			
		PR5	PR6	VNS	MAHM			PR5	PR6	VNS	MAHM
161	87639416.34	0.55	0.39	0.12	**0.00**	181	188328642.01	0.19	0.19	0.02	**0.00**
162	88308655.30	0.52	0.35	0.20	**0.00**	182	188137934.40	0.23	0.23	0.02	**0.00**
163	87383122.46	1.08	0.75	0.11	**0.00**	183	193413641.51	0.12	0.12	**0.00**	**0.00**
164	87603291.09	0.50	0.23	0.03	**0.00**	184	185888714.82	0.13	0.13	0.06	**0.00**
165	87749837.91	0.53	0.23	0.08	**0.00**	185	187717497.96	0.09	0.09	0.06	**0.00**
166	79920046.71	0.63	0.42	0.11	**0.00**	186	169253640.56	0.28	0.28	0.10	**0.00**
167	78286801.64	0.28	0.20	**0.05**	0.08	187	168200456.70	0.34	0.12	0.09	**0.08**
168	80406071.67	0.65	0.47	0.33	**0.09**	188	175172681.29	0.23	0.22	0.06	**0.00**
169	79586125.17	0.58	0.25	**0.01**	0.05	189	164130006.40	**0.17**	0.20	0.28	0.25
170	79275718.38	0.60	0.53	0.35	**0.10**	190	172484674.75	0.35	0.35	0.09	**0.02**
171	90918498.88	0.16	0.08	0.08	**0.02**	191	197873733.40	0.16	0.14	0.03	**0.00**
172	90832351.13	0.22	0.06	0.03	**0.01**	192	196100064.60	0.20	0.17	0.03	**0.02**
173	91913856.33	0.29	0.06	0.06	**0.05**	193	204182428.16	0.08	0.01	0.01	**0.00**
174	89996693.40	0.30	0.16	0.08	**0.01**	194	194202099.66	0.12	0.15	0.07	**0.00**
175	91285081.20	0.18	0.12	0.11	**0.05**	195	198604845.06	0.10	0.10	0.08	**0.05**
176	85892995.03	0.68	0.69	0.15	**0.00**	196	186204546.26	0.25	0.25	0.04	**0.00**
177	86064607.05	0.88	0.84	0.09	**0.00**	197	185840787.55	0.41	0.46	0.03	**0.00**
178	87205216.25	0.64	0.64	0.19	**0.00**	198	191084439.45	0.36	0.36	0.02	**0.00**
179	85396791.04	0.42	0.37	0.18	**0.01**	199	183687347.08	0.25	0.25	0.04	**0.00**
180	87413253.24	0.59	0.59	0.03	**0.00**	200	191866968.77	0.28	0.28	0.11	**0.00**

Table 7. Number of executions for which *PR5* (A), *PR6* (B), *VNS* (C), and *MAHM* (D) has produced the best-found solution

ID	A	B	C	D	ID	A	B	C	D	ID	A	B	C	D	ID	A	B	C	D
Small instances																			
1	0	1	0	0	23	10	10	0	0	45	6	0	0	0	67	0	0	0	1
2	0	0	0	3	24	10	10	0	0	46	0	0	0	1	68	0	0	0	1
3	0	0	0	8	25	7	5	0	0	47	0	0	0	1	69	0	0	0	5
4	2	7	0	0	26	0	0	0	1	48	0	1	0	0	70	0	0	0	1
5	1	1	0	0	27	10	0	0	0	49	1	0	0	0	71	0	7	0	0
6	0	1	0	0	28	0	0	0	8	50	0	0	0	3	72	0	0	0	7
7	0	0	6	0	29	0	0	0	1	51	4	0	0	0	73	0	0	4	10
8	0	0	2	10	30	0	1	0	0	52	1	3	0	0	74	0	0	0	1
9	0	0	3	9	31	0	0	0	1	53	10	0	0	0	75	10	10	10	10
10	0	5	0	0	32	0	0	0	1	54	5	9	0	0	76	1	0	0	0
11	4	0	0	0	33	0	0	0	3	55	2	3	0	0	77	0	0	0	1
12	9	3	0	0	34	0	0	0	2	56	0	1	0	0	78	1	10	0	3
13	0	0	0	3	35	0	0	0	1	57	0	1	0	0	79	10	1	0	0
14	1	0	0	0	36	0	0	10	10	58	0	1	0	0	80	0	0	0	2
15	0	0	0	1	37	0	0	0	1	59	4	8	0	0	81	0	3	0	0
16	1	0	0	0	38	0	0	0	1	60	1	0	0	0	82	0	0	0	2
17	0	2	0	10	39	10	0	0	7	61	0	0	0	3	83	3	0	0	0
18	0	1	0	0	40	2	2	0	0	62	0	0	10	9	84	2	1	0	0
19	0	0	0	1	41	0	0	2	9	63	7	0	0	5	85	0	0	0	1
20	0	1	0	0	42	10	0	0	0	64	10	10	10	10					
21	10	5	0	2	43	0	0	0	1	65	9	0	10	10					
22	1	0	0	0	44	0	0	1	10	66	1	0	0	0					
Medium instances																			
86	0	1	0	0	105	0	0	5	1	124	0	0	0	1	143	0	0	0	1
87	0	0	0	2	106	1	0	0	0	125	0	0	0	1	144	5	10	0	0
88	0	1	0	0	107	0	0	0	1	126	0	1	0	0	145	0	0	0	1
89	0	0	0	2	108	0	3	0	0	127	0	1	0	0	146	0	0	4	10
90	0	0	4	6	109	0	0	1	6	128	0	4	0	0	147	3	0	0	0
91	0	0	0	1	110	0	0	0	1	129	0	1	0	0	148	2	4	0	10
92	0	0	0	1	111	0	0	0	1	130	0	0	0	1	149	0	1	0	0
93	0	0	0	4	112	0	1	0	0	131	0	0	0	1	150	0	0	0	1
94	4	0	0	0	113	0	1	0	0	132	0	0	0	2	151	0	0	0	8
95	0	0	0	4	114	0	0	8	10	133	0	1	0	0	152	0	5	0	0
96	0	0	0	1	115	0	4	0	0	134	0	2	0	0	153	0	0	0	9
97	0	0	0	2	116	0	6	0	0	135	0	5	0	0	154	0	0	0	3
98	0	0	0	5	117	0	0	0	10	136	1	0	0	0	155	10	10	10	10
99	1	8	10	7	118	0	0	0	2	137	0	0	0	1	156	0	0	10	10
100	0	0	0	1	119	0	10	10	10	138	0	0	0	1	157	0	0	10	8
101	0	1	0	0	120	0	0	0	1	139	0	0	0	4	158	0	0	1	9
102	0	0	0	2	121	0	0	0	3	140	0	1	0	0	159	0	0	0	3
103	0	0	0	3	122	0	1	0	0	141	0	1	0	0	160	1	0	0	0
104	0	0	0	5	123	0	0	6	9	142	0	1	0	0					
Large instances																			
161	0	0	0	3	171	0	0	0	3	181	0	0	0	1	191	0	0	0	1
162	0	0	0	10	172	0	2	4	9	182	0	0	4	10	192	0	0	7	2
163	0	0	0	10	173	0	0	2	4	183	0	0	5	10	193	0	0	0	2
164	0	0	0	3	174	0	0	0	9	184	0	0	0	10	194	0	0	0	10
165	0	0	0	10	175	0	0	0	3	185	0	0	0	10	195	0	0	0	2
166	0	0	1	4	176	0	0	1	10	186	0	0	1	10	196	0	0	6	10
167	0	0	6	8	177	0	0	4	10	187	0	2	0	0	197	0	0	6	10
168	0	0	0	6	178	0	0	0	10	188	0	0	0	7	198	0	0	7	10
169	0	0	0	7	179	0	0	0	8	189	1	0	0	0	199	0	0	1	10
170	0	0	0	8	180	0	0	0	2	190	0	0	0	8	200	0	0	0	7

Table 8. Mean results concerning the solution quality for small instances

ID	PR5	PR6	VNS	MAHM	ID	PR5	PR6	VNS	MAHM
1	3.546E+07	**3.542E+07**	3.614E+07	3.612E+07	44	3.733E+07	3.729E+07	3.728E+07	**3.722E+07**
2	3.555E+07	**3.545E+07**	3.641E+07	3.606E+07	45	**3.819E+07**	3.821E+07	3.851E+07	3.842E+07
3	3.582E+07	3.613E+07	3.674E+07	**3.565E+07**	46	3.726E+07	3.726E+07	3.775E+07	**3.716E+07**
4	3.550E+07	**3.544E+07**	3.561E+07	3.555E+07	47	3.789E+07	**3.770E+07**	3.779E+07	3.776E+07
5	3.587E+07	**3.587E+07**	3.645E+07	3.627E+07	48	3.847E+07	**3.844E+07**	3.894E+07	3.868E+07
6	3.308E+07	3.304E+07	3.304E+07	**3.303E+07**	49	**3.679E+07**	3.682E+07	3.740E+07	3.713E+07
7	3.310E+07	3.294E+07	**3.279E+07**	3.289E+07	50	3.763E+07	**3.756E+07**	3.783E+07	3.766E+07
8	3.374E+07	3.358E+07	3.352E+07	**3.336E+07**	51	**4.344E+07**	4.389E+07	4.416E+07	4.416E+07
9	3.272E+07	3.264E+07	3.256E+07	**3.247E+07**	52	**4.387E+07**	4.392E+07	4.398E+07	4.400E+07
10	3.230E+07	**3.223E+07**	3.243E+07	3.246E+07	53	**4.454E+07**	4.454E+07	4.546E+07	4.518E+07
11	**3.572E+07**	3.577E+07	3.617E+07	3.594E+07	54	4.362E+07	**4.360E+07**	4.471E+07	4.450E+07
12	**3.549E+07**	3.550E+07	3.629E+07	3.614E+07	55	**4.395E+07**	4.401E+07	4.420E+07	4.415E+07
13	3.604E+07	3.603E+07	3.609E+07	**3.603E+07**	56	4.117E+07	**4.058E+07**	4.113E+07	4.083E+07
14	**3.506E+07**	3.513E+07	3.534E+07	3.531E+07	57	3.895E+07	**3.894E+07**	4.031E+07	4.004E+07
15	**3.604E+07**	**3.604E+07**	3.612E+07	3.610E+07	58	**4.142E+07**	4.151E+07	4.199E+07	4.170E+07
16	3.533E+07	**3.528E+07**	3.606E+07	3.584E+07	59	3.945E+07	**3.945E+07**	4.023E+07	4.011E+07
17	2.976E+07	2.953E+07	2.985E+07	**2.947E+07**	60	**3.997E+07**	4.001E+07	4.032E+07	4.004E+07
18	2.970E+07	**2.950E+07**	2.975E+07	2.954E+07	61	**4.373E+07**	4.381E+07	4.402E+07	4.383E+07
19	2.988E+07	**2.985E+07**	2.999E+07	2.985E+07	62	4.441E+07	4.441E+07	**4.428E+07**	4.430E+07
20	3.005E+07	3.000E+07	2.987E+07	**2.986E+07**	63	**4.552E+07**	4.553E+07	4.576E+07	4.556E+07
21	**3.128E+07**	3.132E+07	3.149E+07	3.145E+07	64	**4.205E+07**	**4.205E+07**	**4.205E+07**	**4.205E+07**
22	**3.078E+07**	3.085E+07	3.107E+07	3.118E+07	65	4.246E+07	4.247E+07	**4.246E+07**	**4.246E+07**
23	**3.101E+07**	**3.101E+07**	3.110E+07	3.110E+07	66	**4.390E+07**	4.450E+07	4.455E+07	4.448E+07
24	**3.173E+07**	**3.173E+07**	3.190E+07	3.188E+07	67	9.544E+07	9.547E+07	9.603E+07	**9.507E+07**
25	3.097E+07	**3.096E+07**	3.114E+07	3.113E+07	68	9.980E+07	**9.978E+07**	9.994E+07	9.979E+07
26	3.121E+07	**3.120E+07**	3.198E+07	3.186E+07	69	9.276E+07	9.278E+07	9.287E+07	**9.269E+07**
27	**3.099E+07**	3.110E+07	3.163E+07	3.152E+07	70	8.915E+07	8.940E+07	8.918E+07	**8.902E+07**
28	**3.141E+07**	**3.141E+07**	3.165E+07	3.143E+07	71	8.669E+07	**8.642E+07**	8.663E+07	8.663E+07
29	**3.140E+07**	3.158E+07	3.238E+07	3.213E+07	72	8.781E+07	8.746E+07	**8.672E+07**	8.685E+07
30	3.279E+07	**3.242E+07**	3.348E+07	3.321E+07	73	9.069E+07	9.061E+07	9.024E+07	**9.015E+07**
31	3.871E+07	**3.864E+07**	3.880E+07	3.876E+07	74	8.420E+07	8.352E+07	8.353E+07	**8.308E+07**
32	3.811E+07	**3.809E+07**	3.837E+07	3.814E+07	75	**8.493E+07**	**8.493E+07**	**8.493E+07**	**8.493E+07**
33	3.843E+07	**3.842E+07**	3.900E+07	3.859E+07	76	**9.853E+07**	9.871E+07	9.905E+07	9.911E+07
34	**3.846E+07**	3.849E+07	3.888E+07	3.873E+07	77	9.901E+07	9.945E+07	9.928E+07	**9.861E+07**
35	**3.740E+07**	3.742E+07	3.838E+07	3.756E+07	78	1.013E+08	**1.012E+08**	1.012E+08	1.012E+08
36	3.423E+07	3.423E+07	**3.383E+07**	**3.383E+07**	79	**9.487E+07**	9.507E+07	9.552E+07	9.551E+07
37	**3.365E+07**	3.394E+07	3.390E+07	3.394E+07	80	9.487E+07	9.487E+07	9.467E+07	**9.451E+07**
38	3.435E+07	3.435E+07	3.426E+07	**3.425E+07**	81	9.537E+07	**9.388E+07**	9.489E+07	9.469E+07
39	**3.297E+07**	3.297E+07	3.311E+07	3.299E+07	82	9.591E+07	9.593E+07	9.675E+07	**9.558E+07**
40	3.448E+07	**3.443E+07**	3.480E+07	3.469E+07	83	**9.893E+07**	1.009E+08	1.003E+08	1.002E+08
41	3.858E+07	3.858E+07	3.856E+07	**3.855E+07**	84	**9.529E+07**	9.540E+07	9.756E+07	9.643E+07
42	**3.858E+07**	3.862E+07	3.867E+07	3.866E+07	85	**9.001E+07**	9.036E+07	9.036E+07	9.033E+07
43	**3.871E+07**	**3.871E+07**	3.888E+07	3.882E+07					

Table 9. Mean results concerning the solution quality for medium instances

ID	PR5	PR6	VNS	MAHM	ID	PR5	PR6	VNS	MAHM
86	4.757E+07	**4.721E+07**	4.728E+07	4.740E+07	124	5.066E+07	5.035E+07	5.028E+07	**5.016E+07**
87	4.734E+07	4.699E+07	4.689E+07	**4.684E+07**	125	5.075E+07	5.054E+07	5.056E+07	**5.052E+07**
88	4.760E+07	4.721E+07	4.734E+07	**4.706E+07**	126	6.258E+07	**6.247E+07**	6.261E+07	6.247E+07
89	4.715E+07	4.704E+07	4.717E+07	**4.702E+07**	127	6.419E+07	6.430E+07	6.426E+07	**6.413E+07**
90	4.709E+07	4.698E+07	4.679E+07	**4.676E+07**	128	6.434E+07	**6.422E+07**	6.450E+07	6.444E+07
91	5.292E+07	5.285E+07	5.311E+07	**5.283E+07**	129	6.263E+07	**6.251E+07**	6.272E+07	6.270E+07
92	5.276E+07	5.274E+07	5.274E+07	**5.261E+07**	130	6.217E+07	6.211E+07	6.191E+07	**6.190E+07**
93	5.397E+07	5.399E+07	5.386E+07	**5.342E+07**	131	5.729E+07	5.695E+07	5.718E+07	**5.681E+07**
94	**5.164E+07**	5.193E+07	5.244E+07	5.198E+07	132	5.750E+07	5.748E+07	5.779E+07	**5.669E+07**
95	5.263E+07	5.263E+07	5.295E+07	**5.258E+07**	133	5.846E+07	5.845E+07	5.846E+07	**5.826E+07**
96	5.079E+07	5.081E+07	**5.062E+07**	5.063E+07	134	5.682E+07	5.669E+07	5.673E+07	**5.665E+07**
97	5.119E+07	5.108E+07	5.094E+07	**5.085E+07**	135	5.836E+07	**5.809E+07**	5.847E+07	5.834E+07
98	5.198E+07	5.195E+07	5.182E+07	**5.162E+07**	136	**6.612E+07**	6.619E+07	6.639E+07	6.620E+07
99	5.043E+07	5.035E+07	**5.033E+07**	5.040E+07	137	**6.446E+07**	6.466E+07	6.498E+07	6.482E+07
100	5.123E+07	5.115E+07	5.118E+07	**5.109E+07**	138	6.657E+07	6.650E+07	6.689E+07	**6.642E+07**
101	4.503E+07	4.492E+07	4.499E+07	**4.484E+07**	139	**6.438E+07**	**6.438E+07**	6.542E+07	6.469E+07
102	4.541E+07	4.519E+07	4.515E+07	**4.508E+07**	140	6.619E+07	**6.617E+07**	6.669E+07	6.624E+07
103	4.557E+07	4.551E+07	4.562E+07	**4.546E+07**	141	6.253E+07	**6.231E+07**	6.244E+07	6.243E+07
104	4.550E+07	4.537E+07	4.546E+07	**4.529E+07**	142	6.279E+07	**6.255E+07**	6.283E+07	6.284E+07
105	4.417E+07	4.384E+07	**4.360E+07**	4.368E+07	143	6.374E+07	6.368E+07	6.374E+07	**6.346E+07**
106	**4.148E+07**	4.149E+07	4.155E+07	4.154E+07	144	6.085E+07	**6.080E+07**	6.097E+07	6.097E+07
107	4.193E+07	**4.178E+07**	4.203E+07	4.180E+07	145	6.370E+07	6.378E+07	6.379E+07	**6.368E+07**
108	4.182E+07	**4.172E+07**	4.191E+07	4.183E+07	146	1.362E+08	1.361E+08	1.357E+08	**1.355E+08**
109	4.233E+07	4.213E+07	4.175E+07	**4.160E+07**	147	**1.345E+08**	1.345E+08	1.346E+08	1.346E+08
110	4.129E+07	4.115E+07	4.120E+07	**4.104E+07**	148	1.380E+08	1.379E+08	1.382E+08	**1.378E+08**
111	4.611E+07	**4.603E+07**	4.626E+07	4.615E+07	149	**1.329E+08**	1.334E+08	1.333E+08	1.333E+08
112	4.646E+07	**4.640E+07**	4.664E+07	4.651E+07	150	1.165E+08	**1.161E+08**	1.170E+08	1.168E+08
113	**4.669E+07**	4.679E+07	4.699E+07	4.685E+07	151	1.414E+08	1.414E+08	**1.403E+08**	1.403E+08
114	4.683E+07	4.676E+07	4.660E+07	**4.659E+07**	152	1.427E+08	**1.425E+08**	1.432E+08	1.431E+08
115	4.570E+07	**4.549E+07**	4.564E+07	4.563E+07	153	1.476E+08	1.474E+08	1.468E+08	**1.468E+08**
116	4.457E+07	**4.452E+07**	4.462E+07	4.460E+07	154	1.385E+08	1.385E+08	1.386E+08	**1.382E+08**
117	4.417E+07	4.410E+07	4.433E+07	**4.400E+07**	155	**1.364E+08**	**1.364E+08**	**1.364E+08**	**1.364E+08**
118	4.525E+07	**4.515E+07**	4.520E+07	4.519E+07	156	1.327E+08	1.327E+08	**1.324E+08**	**1.324E+08**
119	4.427E+07	**4.421E+07**	**4.421E+07**	**4.421E+07**	157	1.328E+08	1.328E+08	**1.325E+08**	1.326E+08
120	4.368E+07	4.351E+07	4.343E+07	**4.329E+07**	158	1.405E+08	1.400E+08	1.399E+08	**1.398E+08**
121	5.099E+07	5.084E+07	5.067E+07	**5.060E+07**	159	1.319E+08	1.319E+08	1.319E+08	**1.319E+08**
122	5.029E+07	5.026E+07	5.025E+07	**5.011E+07**	160	**1.320E+08**	1.333E+08	1.335E+08	1.333E+08
123	5.065E+07	5.045E+07	5.043E+07	**5.039E+07**					

Table 10. Mean results concerning the solution quality for large instances

ID	PR5	PR6	VNS	MAHM	ID	PR5	PR6	VNS	MAHM
161	8.812E+07	8.798E+07	8.775E+07	**8.764E+07**	181	1.887E+08	1.887E+08	1.884E+08	**1.883E+08**
162	8.876E+07	8.861E+07	8.848E+07	**8.831E+07**	182	1.886E+08	1.886E+08	1.882E+08	**1.881E+08**
163	8.833E+07	8.804E+07	8.748E+07	**8.738E+07**	183	1.936E+08	1.936E+08	1.934E+08	**1.934E+08**
164	8.804E+07	8.780E+07	8.763E+07	**8.760E+07**	184	1.861E+08	1.861E+08	1.860E+08	**1.859E+08**
165	8.822E+07	8.795E+07	8.782E+07	**8.775E+07**	185	1.879E+08	1.879E+08	1.878E+08	**1.877E+08**
166	8.043E+07	8.025E+07	8.001E+07	**7.992E+07**	186	1.697E+08	1.697E+08	1.694E+08	**1.693E+08**
167	7.851E+07	7.844E+07	**7.832E+07**	7.835E+07	187	1.688E+08	1.684E+08	1.683E+08	**1.683E+08**
168	8.093E+07	8.078E+07	8.068E+07	**8.048E+07**	188	1.756E+08	1.756E+08	1.753E+08	**1.752E+08**
169	8.004E+07	7.978E+07	**7.960E+07**	7.962E+07	189	**1.644E+08**	1.645E+08	1.646E+08	1.645E+08
170	7.975E+07	7.970E+07	7.956E+07	**7.936E+07**	190	1.731E+08	1.731E+08	1.726E+08	**1.725E+08**
171	9.106E+07	9.099E+07	9.099E+07	**9.093E+07**	191	1.982E+08	1.982E+08	1.979E+08	**1.979E+08**
172	9.103E+07	9.089E+07	9.086E+07	**9.084E+07**	192	1.965E+08	1.964E+08	1.962E+08	**1.961E+08**
173	9.218E+07	9.197E+07	9.197E+07	**9.196E+07**	193	2.043E+08	2.042E+08	2.042E+08	**2.042E+08**
174	9.027E+07	9.014E+07	9.007E+07	**9.000E+07**	194	1.944E+08	1.945E+08	1.943E+08	**1.942E+08**
175	9.145E+07	9.140E+07	9.138E+07	**9.133E+07**	195	1.988E+08	1.988E+08	1.988E+08	**1.987E+08**
176	8.648E+07	8.648E+07	8.602E+07	**8.589E+07**	196	1.867E+08	1.867E+08	1.863E+08	**1.862E+08**
177	8.682E+07	8.679E+07	8.614E+07	**8.606E+07**	197	1.866E+08	1.867E+08	1.859E+08	**1.858E+08**
178	8.777E+07	8.777E+07	8.737E+07	**8.721E+07**	198	1.918E+08	1.918E+08	1.911E+08	**1.911E+08**
179	8.576E+07	8.571E+07	8.555E+07	**8.541E+07**	199	1.841E+08	1.841E+08	1.838E+08	**1.837E+08**
180	8.793E+07	8.793E+07	8.744E+07	**8.741E+07**	200	1.924E+08	1.924E+08	1.921E+08	**1.919E+08**

Table 11. Median results concerning the solution quality for small instances

ID	PR5	PR6	VNS	MAHM	ID	PR5	PR6	VNS	MAHM
1	3.55E+07	**3.54E+07**	3.61E+07	3.61E+07	44	3.731E+07	3.729E+07	3.729E+07	**3.722E+07**
2	3.55E+07	**3.54E+07**	3.64E+07	3.63E+07	45	**3.818E+07**	3.821E+07	3.851E+07	3.842E+07
3	3.56E+07	3.61E+07	3.67E+07	**3.54E+07**	46	**3.726E+07**	**3.726E+07**	3.776E+07	3.758E+07
4	3.55E+07	**3.54E+07**	3.56E+07	3.55E+07	47	3.798E+07	**3.762E+07**	3.779E+07	3.779E+07
5	**3.59E+07**	3.59E+07	3.65E+07	3.64E+07	48	3.847E+07	**3.845E+07**	3.894E+07	3.864E+07
6	3.31E+07	**3.30E+07**	**3.30E+07**	**3.30E+07**	49	**3.684E+07**	3.688E+07	3.740E+07	3.707E+07
7	3.31E+07	3.29E+07	**3.28E+07**	3.29E+07	50	3.758E+07	**3.758E+07**	3.786E+07	3.769E+07
8	3.38E+07	3.36E+07	3.36E+07	**3.34E+07**	51	**4.339E+07**	4.387E+07	4.416E+07	4.416E+07
9	3.27E+07	3.26E+07	3.26E+07	**3.25E+07**	52	**4.378E+07**	4.398E+07	4.398E+07	4.397E+07
10	3.22E+07	**3.22E+07**	3.24E+07	3.24E+07	53	**4.454E+07**	4.454E+07	4.544E+07	4.527E+07
11	**3.57E+07**	3.57E+07	3.62E+07	3.59E+07	54	4.362E+07	**4.360E+07**	4.472E+07	4.450E+07
12	**3.55E+07**	3.55E+07	3.63E+07	3.62E+07	55	**4.395E+07**	4.408E+07	4.420E+07	4.420E+07
13	**3.60E+07**	**3.60E+07**	3.61E+07	3.61E+07	56	4.127E+07	**4.055E+07**	4.109E+07	4.084E+07
14	**3.51E+07**	3.52E+07	3.53E+07	3.53E+07	57	**3.895E+07**	**3.895E+07**	4.030E+07	4.007E+07
15	**3.60E+07**	**3.60E+07**	3.61E+07	3.61E+07	58	**4.142E+07**	4.166E+07	4.200E+07	4.169E+07
16	3.53E+07	**3.53E+07**	3.61E+07	3.59E+07	59	3.946E+07	**3.942E+07**	4.024E+07	4.021E+07
17	2.97E+07	2.95E+07	2.99E+07	**2.95E+07**	60	**3.997E+07**	4.001E+07	4.032E+07	4.004E+07
18	2.97E+07	2.96E+07	2.98E+07	**2.95E+07**	61	**4.371E+07**	4.381E+07	4.402E+07	4.393E+07
19	2.99E+07	**2.98E+07**	3.00E+07	2.99E+07	62	4.441E+07	4.441E+07	**4.428E+07**	**4.428E+07**
20	3.00E+07	3.00E+07	2.99E+07	**2.98E+07**	63	**4.552E+07**	4.553E+07	4.576E+07	4.556E+07
21	**3.13E+07**	3.13E+07	3.15E+07	3.15E+07	64	**4.205E+07**	**4.205E+07**	**4.205E+07**	**4.205E+07**
22	**3.08E+07**	3.09E+07	3.11E+07	3.12E+07	65	**4.246E+07**	4.247E+07	**4.246E+07**	**4.246E+07**
23	**3.10E+07**	**3.10E+07**	3.11E+07	3.11E+07	66	**4.384E+07**	4.450E+07	4.454E+07	4.450E+07
24	**3.17E+07**	**3.17E+07**	3.19E+07	3.19E+07	67	9.547E+07	**9.547E+07**	9.603E+07	9.565E+07
25	**3.09E+07**	3.10E+07	3.11E+07	3.11E+07	68	9.978E+07	9.978E+07	9.994E+07	**9.973E+07**
26	3.12E+07	**3.12E+07**	3.20E+07	3.20E+07	69	9.270E+07	9.275E+07	9.292E+07	**9.269E+07**
27	**3.10E+07**	3.11E+07	3.16E+07	3.15E+07	70	8.940E+07	8.940E+07	**8.918E+07**	**8.918E+07**
28	3.14E+07	3.14E+07	3.16E+07	**3.14E+07**	71	8.672E+07	**8.635E+07**	8.663E+07	8.663E+07
29	**3.14E+07**	3.16E+07	3.24E+07	3.24E+07	72	8.821E+07	8.744E+07	8.671E+07	**8.640E+07**
30	3.29E+07	**3.24E+07**	3.35E+07	3.33E+07	73	9.055E+07	9.055E+07	9.016E+07	**9.015E+07**
31	3.87E+07	**3.86E+07**	3.88E+07	3.88E+07	74	8.432E+07	**8.349E+07**	8.353E+07	8.353E+07
32	**3.81E+07**	**3.81E+07**	3.84E+07	3.83E+07	75	**8.493E+07**	**8.493E+07**	**8.493E+07**	**8.493E+07**
33	3.84E+07	**3.84E+07**	3.90E+07	3.85E+07	76	**9.855E+07**	9.871E+07	9.902E+07	9.913E+07
34	**3.85E+07**	3.85E+07	3.89E+07	3.89E+07	77	**9.901E+07**	9.945E+07	9.928E+07	9.928E+07
35	**3.74E+07**	3.74E+07	3.84E+07	3.79E+07	78	1.013E+08	**1.012E+08**	1.012E+08	1.012E+08
36	3.42E+07	3.42E+07	**3.38E+07**	**3.38E+07**	79	**9.487E+07**	9.509E+07	9.551E+07	9.551E+07
37	**3.36E+07**	3.39E+07	3.39E+07	3.39E+07	80	9.487E+07	9.487E+07	9.467E+07	**9.463E+07**
38	3.43E+07	3.43E+07	**3.43E+07**	**3.43E+07**	81	9.542E+07	**9.379E+07**	9.483E+07	9.483E+07
39	**3.30E+07**	3.30E+07	3.31E+07	**3.30E+07**	82	9.594E+07	9.594E+07	9.675E+07	**9.561E+07**
40	3.44E+07	**3.44E+07**	3.48E+07	3.47E+07	83	**9.888E+07**	1.009E+08	1.002E+08	1.001E+08
41	3.86E+07	3.86E+07	3.86E+07	**3.85E+07**	84	**9.533E+07**	**9.533E+07**	9.756E+07	9.632E+07
42	**3.86E+07**	3.86E+07	3.87E+07	3.87E+07	85	**9.001E+07**	9.036E+07	9.036E+07	9.036E+07
43	**3.87E+07**	**3.87E+07**	3.89E+07	3.89E+07					

Table 12. Median results concerning the solution quality for medium instances

ID	PR5	PR6	VNS	MAHM	ID	PR5	PR6	VNS	MAHM
86	4.760E+07	**4.717E+07**	4.727E+07	4.748E+07	124	5.068E+07	5.027E+07	5.017E+07	**5.016E+07**
87	4.737E+07	4.694E+07	4.687E+07	**4.684E+07**	125	5.075E+07	5.056E+07	5.056E+07	**5.050E+07**
88	4.772E+07	4.725E+07	4.731E+07	**4.703E+07**	126	6.263E+07	6.248E+07	6.261E+07	**6.247E+07**
89	4.716E+07	**4.704E+07**	4.721E+07	4.704E+07	127	6.425E+07	6.438E+07	6.425E+07	**6.411E+07**
90	4.712E+07	4.698E+07	4.678E+07	**4.675E+07**	128	6.437E+07	**6.417E+07**	6.450E+07	6.445E+07
91	5.292E+07	5.293E+07	5.311E+07	**5.282E+07**	129	6.265E+07	**6.249E+07**	6.272E+07	6.272E+07
92	5.274E+07	5.274E+07	5.274E+07	**5.265E+07**	130	6.219E+07	6.211E+07	**6.191E+07**	**6.191E+07**
93	5.398E+07	5.408E+07	5.386E+07	**5.355E+07**	131	5.730E+07	**5.696E+07**	5.719E+07	5.717E+07
94	**5.163E+07**	5.192E+07	5.244E+07	5.192E+07	132	5.750E+07	5.748E+07	5.779E+07	**5.735E+07**
95	5.263E+07	5.263E+07	5.291E+07	**5.250E+07**	133	5.848E+07	5.851E+07	5.846E+07	**5.823E+07**
96	5.075E+07	5.075E+07	5.059E+07	**5.058E+07**	134	5.682E+07	5.682E+07	5.675E+07	**5.664E+07**
97	5.120E+07	5.107E+07	5.092E+07	**5.088E+07**	135	5.832E+07	**5.808E+07**	5.846E+07	5.833E+07
98	5.196E+07	5.196E+07	5.180E+07	**5.160E+07**	136	6.630E+07	**6.617E+07**	6.639E+07	6.632E+07
99	5.043E+07	**5.033E+07**	**5.033E+07**	**5.033E+07**	137	**6.442E+07**	6.466E+07	6.500E+07	6.493E+07
100	5.122E+07	5.115E+07	5.119E+07	**5.112E+07**	138	6.660E+07	**6.646E+07**	6.689E+07	6.659E+07
101	4.500E+07	4.498E+07	4.501E+07	**4.487E+07**	139	**6.438E+07**	**6.438E+07**	6.542E+07	6.458E+07
102	4.537E+07	4.521E+07	4.511E+07	**4.510E+07**	140	6.623E+07	**6.620E+07**	6.668E+07	6.636E+07
103	4.558E+07	4.548E+07	4.561E+07	**4.542E+07**	141	6.257E+07	**6.232E+07**	6.244E+07	6.243E+07
104	4.557E+07	4.536E+07	4.545E+07	**4.529E+07**	142	6.280E+07	**6.252E+07**	6.283E+07	6.283E+07
105	4.415E+07	4.384E+07	**4.357E+07**	4.368E+07	143	6.370E+07	6.369E+07	6.377E+07	**6.348E+07**
106	**4.146E+07**	4.149E+07	4.154E+07	4.156E+07	144	6.084E+07	**6.080E+07**	6.097E+07	6.097E+07
107	4.193E+07	**4.176E+07**	4.202E+07	4.178E+07	145	**6.365E+07**	6.378E+07	6.379E+07	6.372E+07
108	4.181E+07	**4.169E+07**	4.191E+07	4.181E+07	146	1.362E+08	1.363E+08	1.356E+08	**1.355E+08**
109	4.232E+07	4.213E+07	4.168E+07	**4.157E+07**	147	**1.345E+08**	**1.345E+08**	1.346E+08	1.346E+08
110	4.130E+07	4.118E+07	4.116E+07	**4.102E+07**	148	1.380E+08	1.379E+08	1.382E+08	**1.378E+08**
111	4.613E+07	**4.603E+07**	4.625E+07	4.617E+07	149	**1.329E+08**	1.337E+08	1.333E+08	1.333E+08
112	4.649E+07	**4.643E+07**	4.664E+07	4.661E+07	150	1.165E+08	**1.161E+08**	1.170E+08	1.170E+08
113	**4.669E+07**	4.676E+07	4.698E+07	4.683E+07	151	1.414E+08	1.414E+08	1.403E+08	**1.402E+08**
114	4.682E+07	4.675E+07	**4.659E+07**	**4.659E+07**	152	1.427E+08	**1.424E+08**	1.432E+08	1.432E+08
115	4.573E+07	4.547E+07	**4.564E+07**	4.563E+07	153	1.476E+08	1.476E+08	1.468E+08	**1.467E+08**
116	4.457E+07	4.450E+07	**4.460E+07**	4.460E+07	154	**1.385E+08**	**1.385E+08**	1.386E+08	1.385E+08
117	4.416E+07	4.410E+07	4.433E+07	**4.400E+07**	155	**1.364E+08**	**1.364E+08**	**1.364E+08**	**1.364E+08**
118	4.526E+07	**4.515E+07**	4.521E+07	4.518E+07	156	1.328E+08	1.327E+08	**1.324E+08**	**1.324E+08**
119	4.428E+07	4.421E+07	4.421E+07	4.421E+07	157	1.328E+08	1.328E+08	**1.325E+08**	**1.325E+08**
120	4.367E+07	4.352E+07	4.343E+07	**4.331E+07**	158	1.405E+08	1.399E+08	1.398E+08	**1.398E+08**
121	5.104E+07	5.083E+07	5.062E+07	**5.061E+07**	159	**1.319E+08**	**1.319E+08**	**1.319E+08**	**1.319E+08**
122	5.026E+07	5.028E+07	5.021E+07	**5.011E+07**	160	**1.320E+08**	1.333E+08	1.335E+08	1.333E+08
123	5.067E+07	5.044E+07	**5.039E+07**	**5.039E+07**					

Table 13. Median results concerning the solution quality for large instances

ID	PR5	PR6	VNS	MAHM	ID	PR5	PR6	VNS	MAHM
161	8.81E+07	8.80E+07	8.78E+07	**8.76E+07**	181	1.89E+08	1.89E+08	**1.88E+08**	**1.88E+08**
162	8.88E+07	8.86E+07	8.85E+07	**8.83E+07**	182	1.89E+08	1.89E+08	1.88E+08	**1.88E+08**
163	8.84E+07	8.80E+07	8.75E+07	**8.74E+07**	183	1.94E+08	1.94E+08	1.93E+08	**1.93E+08**
164	8.81E+07	8.78E+07	8.76E+07	**8.76E+07**	184	1.86E+08	1.86E+08	1.86E+08	**1.86E+08**
165	8.82E+07	8.80E+07	8.78E+07	**8.77E+07**	185	1.88E+08	1.88E+08	1.88E+08	**1.88E+08**
166	8.04E+07	8.02E+07	8.00E+07	**7.99E+07**	186	1.70E+08	1.70E+08	1.69E+08	**1.69E+08**
167	7.85E+07	7.85E+07	**7.83E+07**	**7.83E+07**	187	1.69E+08	1.68E+08	1.68E+08	**1.68E+08**
168	8.09E+07	8.08E+07	8.07E+07	**8.04E+07**	188	1.76E+08	1.76E+08	1.75E+08	**1.75E+08**
169	8.01E+07	7.97E+07	7.96E+07	**7.96E+07**	189	**1.64E+08**	**1.64E+08**	1.65E+08	1.65E+08
170	7.98E+07	7.98E+07	7.95E+07	**7.93E+07**	190	1.73E+08	1.73E+08	1.73E+08	**1.72E+08**
171	9.11E+07	9.10E+07	9.10E+07	**9.09E+07**	191	1.98E+08	1.98E+08	1.98E+08	**1.98E+08**
172	9.10E+07	9.09E+07	9.08E+07	**9.08E+07**	192	1.97E+08	1.96E+08	**1.96E+08**	1.96E+08
173	9.22E+07	**9.20E+07**	9.20E+07	9.20E+07	193	2.04E+08	2.04E+08	**2.04E+08**	**2.04E+08**
174	9.03E+07	9.01E+07	9.01E+07	**9.00E+07**	194	1.94E+08	1.94E+08	1.94E+08	**1.94E+08**
175	9.14E+07	9.14E+07	9.14E+07	**9.13E+07**	195	1.99E+08	1.99E+08	1.99E+08	**1.99E+08**
176	8.65E+07	8.65E+07	8.60E+07	**8.59E+07**	196	1.87E+08	1.87E+08	**1.86E+08**	**1.86E+08**
177	8.68E+07	8.69E+07	8.61E+07	**8.61E+07**	197	1.87E+08	1.87E+08	**1.86E+08**	**1.86E+08**
178	8.78E+07	8.78E+07	8.74E+07	**8.72E+07**	198	1.92E+08	1.92E+08	**1.91E+08**	**1.91E+08**
179	8.57E+07	8.57E+07	8.55E+07	**8.54E+07**	199	1.84E+08	1.84E+08	1.84E+08	**1.84E+08**
180	8.79E+07	8.79E+07	8.74E+07	**8.74E+07**	200	1.92E+08	1.92E+08	1.92E+08	**1.92E+08**

Table 14. Standard deviation concerning the solution quality for small instances

ID	PR5	PR6	VNS	MAHM	ID	PR5	PR6	VNS	MAHM
1	67189.20	59619.20	**7283.96**	37385.82	44	59918.64	**0.00**	23288.23	**0.00**
2	76941.06	75887.70	**0.00**	441722.09	45	17011.29	**0.00**	**0.00**	107738.76
3	319380.25	93150.71	**60885.72**	554065.63	46	7177.22	5827.20	**5532.65**	1473905.31
4	56591.09	55833.89	41668.22	**40556.92**	47	117251.09	117720.34	**0.00**	62516.25
5	69127.42	38623.59	**0.00**	218442.98	48	24121.10	25463.52	**0.00**	175863.03
6	66974.13	8158.29	8158.29	**0.00**	49	94745.80	102657.29	**0.00**	205907.86
7	107418.80	32754.08	35916.84	**22203.76**	50	66950.69	**27202.61**	48749.82	169455.71
8	47186.66	**0.00**	82925.75	**0.00**	51	160844.65	127369.96	**0.00**	**0.00**
9	69170.91	**3382.76**	76100.11	23065.63	52	125519.13	116002.47	**0.00**	124098.00
10	121995.96	**3872.04**	34373.77	146145.00	53	**0.00**	**0.00**	42542.98	224789.96
11	15904.33	66450.26	**0.00**	115003.82	54	**18328.94**	18571.84	22117.05	153667.13
12	**1463.81**	11595.46	9417.39	176890.64	55	60105.54	99695.58	**0.00**	96818.43
13	29635.82	22226.86	**0.00**	93286.99	56	242044.17	166803.05	54582.41	**32736.44**
14	78987.40	77199.89	**0.00**	71087.46	57	23355.77	20152.79	**11860.63**	101855.16
15	**0.00**	**0.00**	10114.41	55739.57	58	**1563.55**	203558.83	17959.28	14426.85
16	62979.21	**0.00**	**0.00**	180911.43	59	28091.72	75755.04	**13801.86**	184298.55
17	123564.33	93483.98	115175.64	**0.00**	60	152829.63	**0.00**	**0.00**	750.72
18	108098.51	184952.76	**65432.19**	81830.44	61	23782.56	**0.00**	**0.00**	186340.47
19	37014.45	**17700.67**	27045.54	118403.15	62	**0.00**	**0.00**	**0.00**	40769.80
20	**26932.34**	132380.36	52283.95	134782.18	63	4494.22	**0.00**	**0.00**	38658.59
21	**0.00**	35565.69	0.00	84713.08	64	**0.00**	**0.00**	**0.00**	**0.00**
22	47249.66	49345.02	**0.00**	138950.58	65	1090.87	**0.00**	**0.00**	**0.00**
23	**0.00**	**0.00**	**0.00**	**0.00**	66	164266.23	**0.00**	30695.18	52023.06
24	**0.00**	**0.00**	**0.00**	49086.56	67	95944.27	**0.00**	**0.00**	1934869.71
25	84802.66	28120.92	**0.00**	5616.71	68	58451.00	9545.09	**0.00**	104435.70
26	9116.98	**0.00**	**0.00**	483856.97	69	124991.89	123829.94	**60253.23**	116933.56
27	**0.00**	**0.00**	**0.00**	75118.42	70	529358.69	**0.00**	**0.00**	408384.10
28	**0.00**	**0.00**	76295.62	157476.16	71	59900.05	110016.71	**0.00**	**0.00**
29	80474.50	3089.82	**0.00**	539029.46	72	606143.46	360416.04	**46332.45**	725492.88
30	328417.74	63626.73	**11162.35**	279928.60	73	190088.12	66157.49	142680.06	**0.00**
31	111865.23	2343.17	**0.00**	185328.39	74	196239.86	362698.72	**0.00**	1392552.82
32	35126.47	**26881.08**	50792.97	237133.10	75	**0.00**	**0.00**	**0.00**	**0.00**
33	48817.60	8640.39	**2438.28**	294451.97	76	191677.83	**0.00**	52249.40	45607.02
34	23088.86	**0.00**	15174.80	203871.33	77	**0.00**	**0.00**	**0.00**	2127673.71
35	69656.99	**0.00**	14997.95	1340059.85	78	15069.43	**0.00**	**0.00**	**0.00**
36	**0.00**	**0.00**	**0.00**	**0.00**	79	**0.00**	67166.97	18978.22	1045.04
37	57473.19	**1346.71**	11270.36	188120.75	80	**0.00**	**0.00**	38423.69	330538.44
38	9568.04	**5415.67**	23338.88	25186.50	81	**79047.22**	273818.48	173105.51	253996.30
39	0.00	**0.00**	14257.22	22597.46	82	40000.13	25036.61	**0.00**	459291.24
40	167483.07	151006.24	24751.16	**0.00**	83	251969.74	**0.00**	94190.54	237982.64
41	11150.63	**6690.38**	11974.35	38358.57	84	47377.21	248542.09	**0.00**	362959.13
42	**0.00**	**0.00**	4480.04	24052.13	85	**0.00**	**0.00**	**0.00**	114786.52
43	**0.00**	**0.00**	**0.00**	116480.49					

Table 15. Standard deviation concerning the solution quality for medium instances

ID	PR5	PR6	VNS	MAHM	ID	PR5	PR6	VNS	MAHM
86	156959.51	106910.72	**94254.17**	135821.53	124	88483.03	162970.90	156659.19	**13252.66**
87	137762.32	111452.00	60618.31	**0.00**	125	89143.47	29554.63	**22420.05**	32581.42
88	192587.94	174406.31	**64873.30**	86363.49	126	122244.48	111311.72	**0.00**	10344.18
89	**62547.68**	65555.30	87695.65	84529.22	127	248372.65	216159.73	**17761.56**	83390.93
90	53279.11	54948.24	48350.85	**22016.34**	128	57955.79	102396.67	**16135.62**	58079.32
91	16833.73	171191.37	**0.00**	207741.03	129	49455.32	37661.03	**0.00**	41120.45
92	29028.96	**0.00**	**0.00**	114278.57	130	40685.12	**0.00**	**0.00**	15100.20
93	119815.92	174794.55	**8019.64**	245493.54	131	66689.56	90257.05	**8479.99**	1136755.19
94	23001.44	**11161.86**	32901.63	111366.48	132	6508.62	14755.69	**0.00**	1373555.34
95	**0.00**	6316.59	47037.04	169461.48	133	59450.42	165583.81	**21959.28**	62797.97
96	**61750.17**	67312.23	70333.52	87145.01	134	**8364.81**	184483.26	53480.30	99630.93
97	**36912.71**	32030.92	43820.07	57276.96	135	124522.21	39991.28	33136.20	**18982.54**
98	27946.62	**37757.26**	26090.79	35750.99	136	280231.12	39758.40	**0.00**	249779.90
99	67860.21	36990.33	**0.00**	136502.16	137	102242.41	**0.00**	29366.89	208314.12
100	41008.79	**5284.32**	22295.99	113525.93	138	104095.33	87684.66	**13854.41**	484853.34
101	169540.06	276380.13	**43995.86**	104378.69	139	**0.00**	**0.00**	**0.00**	427884.13
102	120428.51	**49371.29**	80406.59	57808.17	140	132056.98	175950.37	**18516.15**	225603.14
103	60934.03	103986.64	**28131.08**	95521.92	141	145429.33	30282.36	2856.34	**0.00**
104	93738.67	7031.90	74226.58	**1017.08**	142	95710.62	100912.58	**0.00**	46097.25
105	112434.14	**9284.05**	54486.97	38157.21	143	92865.62	141804.89	155644.32	**63048.28**
106	119762.17	68126.47	**41451.75**	49317.64	144	56489.74	0.00	**0.00**	0.00
107	66915.83	54460.06	**31446.96**	75867.79	145	129134.96	66525.23	**46539.16**	147327.86
108	136628.92	**61081.40**	69158.52	62661.96	146	260987.68	217380.33	223262.41	**0.00**
109	**50025.75**	87281.06	175486.50	53763.34	147	225426.79	**0.00**	25055.25	96769.55
110	103626.75	115814.92	**68271.31**	106263.80	148	139062.62	103812.23	**0.00**	**0.00**
111	61047.92	38241.73	**14737.44**	88653.63	149	30007.65	412056.84	**0.00**	**0.00**
112	36377.75	99685.51	**0.00**	159277.78	150	327459.94	**46727.82**	128632.47	524524.46
113	60974.80	169331.55	**35685.02**	121177.37	151	**0.00**	**0.00**	146078.31	371751.37
114	69599.69	22413.62	24076.70	**0.00**	152	**0.00**	114968.98	69736.13	86381.09
115	56672.92	63909.51	3316.35	**0.00**	153	40323.09	249826.16	**12822.80**	284412.86
116	25874.68	32951.53	35409.17	**0.00**	154	**10203.73**	58352.93	52856.94	856999.23
117	49984.06	21748.41	40513.91	**0.00**	155	**0.00**	**0.00**	**0.00**	**0.00**
118	80966.23	**21555.09**	27378.31	90472.81	156	47065.68	17276.58	**0.00**	**0.00**
119	14509.25	**0.00**	**0.00**	**0.00**	157	**0.00**	**0.00**	**0.00**	83001.03
120	41129.40	**22706.08**	23500.95	55877.72	158	104096.92	147442.14	116729.35	**96065.45**
121	114727.96	96779.07	**77824.00**	110387.29	159	**0.00**	**0.00**	**0.00**	8749.75
122	**87579.56**	207630.80	92254.05	125398.13	160	**73420.68**	122416.13	121219.04	146514.46
123	70369.07	54071.91	80490.52	**22182.62**					

Table 16. Standard deviation concerning the solution quality for large instances

ID	PR5	PR6	VNS	MAHM	ID	PR5	PR6	VNS	MAHM
161	85187.11	97218.88	58981.33	**0.00**	181	**0.00**	**0.00**	58519.85	**0.00**
162	52604.53	77339.55	57189.96	**0.00**	182	**0.00**	**0.00**	36479.21	**0.00**
163	129861.76	185978.91	58733.38	**0.00**	183	**0.00**	**0.00**	3886.24	**0.00**
164	67398.94	48882.09	51446.92	**0.00**	184	**0.00**	**0.00**	24527.51	**0.00**
165	86653.74	23720.28	46248.85	**0.00**	185	**0.00**	**0.00**	17635.84	**0.00**
166	38822.94	128299.53	66145.22	**0.00**	186	**0.00**	**0.00**	62580.45	**0.00**
167	**5960.66**	62394.75	54641.46	133911.38	187	87372.27	189650.41	**74863.77**	83637.26
168	57857.15	80992.40	**43728.93**	102153.26	188	**0.00**	60252.09	12535.53	**0.00**
169	124936.00	169854.56	**13306.16**	122707.13	189	103857.67	**0.00**	33492.62	35017.60
170	**0.00**	80935.52	94546.63	174623.24	190	**0.00**	**0.00**	42126.73	69439.40
171	36688.21	42279.54	38263.15	**17065.40**	191	16182.99	26971.65	40180.62	**0.00**
172	103296.82	55393.23	37559.70	**37045.81**	192	50563.95	**0.00**	83809.80	35959.69
173	61090.97	59690.64	40933.66	**39106.69**	193	130092.93	**0.00**	24816.67	**0.00**
174	84237.77	112081.99	29748.71	**24403.53**	194	74557.64	**0.00**	20644.32	**0.00**
175	56507.49	54688.44	**11799.78**	32772.48	195	**0.00**	**0.00**	22513.65	48932.89
176	70686.08	93162.66	58170.41	**0.00**	196	**0.00**	**0.00**	91991.23	**0.00**
177	58029.42	119853.98	89566.78	**0.00**	197	147069.77	**0.00**	84840.70	**0.00**
178	**0.00**	**0.00**	57831.43	**0.00**	198	**0.00**	**0.00**	103660.19	**0.00**
179	73872.38	72627.00	30954.47	**17492.86**	199	**0.00**	**0.00**	53723.23	**0.00**
180	**0.00**	**0.00**	20260.46	**0.00**	200	**0.00**	**0.00**	115710.77	5871.28